Available online at www.sciencedirect.com
SCIENCE DIRECT®
ELSEVIER
Palaeogeography, Palaeoclimatology, Palaeoecology xx (2005) xxx–xxx
PALAEO
www.elsevier.com/locate/palaeo

Ecosystem and paleohydrological response to Quaternary climate change in the Bonneville Basin, Utah

Deborah P. Balch[a], Andrew S. Cohen[a,*], Douglas W. Schnurrenberger[b], Brian J. Haskell[c], Blas L. Valero Garces[d], J. Warren Beck[e], Hai Cheng[f], R. Lawrence Edwards[f]

[a]*Department of Geosciences, University of Arizona, Tucson, AZ 85721, United States*
[b]*National Lacustrine Core Repository, University of Minnesota, Minneapolis, MN 55455, United States*
[c]*Limnological Research Center, University of Minnesota, Minneapolis, MN 55455-0219, United States*
[d]*Instituto Pirenaico de Ecologia (Pyrenean Institute of Ecology), Consejo Superior de Investigaciones Cientificas (CSIC), Apdo 202, 50080 Zaragoza, Spain*
[e]*NSF-Arizona Accelerator Mass Spectrometry Facility, Department of Physics, University of Arizona, Tucson, AZ 85721, United States*
[f]*Minnesota Isotope Laboratory, Department of Geology and Geophysics University of Minnesota, Minneapolis, MN 55455, United States*

Received 5 July 2004; received in revised form 9 January 2005; accepted 24 January 2005

Abstract

We report the results of a detailed paleoecological study of the Bonneville basin covering the last ~280,000 yr. Our study used fossil ostracodes and a sedimentological record obtained from the August 2000 GLAD800 drilling operation at Great Salt Lake. We analyzed 125 samples, taken at ~1 m intervals from Site 4 (GSL00-4), for ostracodes and other paleoecologic and sedimentologic indicators of environmental change. Multivariate analyses applied to the ostracode data and qualitative analyses of fossil and sedimentological data indicate an alternation between three major environments at the core site over the cored interval: (1) shallow saline or hypersaline lakes; (2) salt or freshwater marshes; and (3) occasional deep freshwater lakes. These environmental changes are consistent with shoreline studies of regional lake level fluctuations, but provide considerable new detail on both the timing and environmental conditions associated with the various lake phases. Our age model (using ^{14}C, U-series, tephra and biostratigraphic chronologies) allowed us to associate the core's record of regional paleohydrology with the marine oxygen isotope stages of global climate change. The core contains continuous records for the last four glacial/interglacial sequences. Salt/freshwater marshes were common during the interglacials and deep freshwater conditions correspond with maximum global ice volume in OIS 2, and before a maximum in global ice during OIS 6. Immediately following deep lake phases, crashes in lake level from rapid desiccation resulted in the deposition of thick evaporite units. Our study suggests that the climate of the Great Salt Lake catchment appears to have been drier during OIS 6 than during OIS 2.We compare our record of environmental change during OIS 6 glaciation with other records from the western United States and find that the overall

* Corresponding author. Fax: +1 520 621 2672.
E-mail address: acohen@geo.arizona.edu (A.S. Cohen).

0031-0182/$ - see front matter
doi:10.1016/j.palaeo.2005.01.013

pattern of climate was similar throughout the West, but differences in the timing of climate change (i.e. when a region became drier or moister) are common.

Keywords: Paleoclimate; Ostracode; Paleolimnology; Great Salt Lake; Lake Bonneville

1. Introduction

In the late 1990s, the International Continental Drilling Program (ICDP) provided funds for DOSECC (the US nonprofit research consortium for continental scientific drilling) to develop a dedicated lake drilling system, designated the GLAD800 system. The intent of this grant was to jump start scientific drilling in lakes around the world with an inexpensive and modular system that would be easily transported between sites, and would be broadly accessible to the scientific community. This system, including a barge platform, drill rig and coring tool kit, was first tested with NSF support at the Great Salt Lake and Bear Lake in August 2000. The mandate from NSF was that all engineering tests of the GLAD-800 system be coupled to significant scientific questions, so that the testing would also yield scientific benefits. The long history of scientific (and specifically paleoclimate) research on the Great Salt Lake, coupled with DOSECC's location in Salt Lake City, made the Great Salt Lake and Bear Lake natural targets for this testing.

The drilling campaign collected four long cores from the Great Salt Lake and obtained a total of 371 m of sediment with 96% recovery. One site in particular, GSL00-4 (also known as Site 4), reached 121 m below lake floor (mblf) and provides the longest continuous record of the lake's history ever collected from a drilling operation. Drilling took place in the hanging wall of the Carrington Fault, which is located along the southeast margin of the lake's northern basin (Fig. 1). The primary objective for drilling at this site was to obtain a detailed basinal history extending back to Oxygen Isotope Stage (OIS) 6 and to use its paleontological and sedimentological contents to address questions related to paleoclimate. A preliminary study of the core, based on core catcher samples taken every 3 m (ca. 6000 yr resolution), suggested that Site 4 contains a high-resolution paleoecological record extending back ~250,000 yr BP based on tephra correlation and preliminary U-series dating (Dean et al., 2002). Paleoecological analyses of its ostracode assemblages, in particular, have shown that the lake levels have fluctuated over time giving rise to both marsh conditions and saline, open water conditions at the core site (Kowalewska and Cohen, 1998; Dean et al., 2002). Up to this point, we did not have detailed knowledge about these environmental fluctuations because the previous studies were at too low of a resolution. The goal of this current study was to explain these patterns in greater detail by accomplishing the following: (i) increase sampling frequency to improve resolution; (ii) resolve the chronological sequence of paleoecological and paleolimnological change through the acquisition of a reliable age model; and (iii) determine if these changes are correlated with changes in regional or global climate change, particularly at the glacial/interglacial time scale.

1.1. Previous research

The Bonneville basin, located in the northeastern Great Basin, has been a major focus of North American Quaternary research for more than a century. G.K. Gilbert (1890) was the first to recognize that the basin contains excellent stratigraphic records of past environmental change. By studying its lacustrine deposits, he reconstructed the history of Lake Bonneville, emphasizing its dramatic transgressions and regressions during the late Pleistocene. In 1948, Ernst Antevs proposed a correlation between the maximum height of Lake Bonneville and the maximum extent of the North American ice sheet during the late Pleistocene (Antevs, 1948; Oviatt, 2002).

Research in the late 20th Century has provided evidence that at least four deep lake cycles have occurred in the Bonneville basin over the past 500,000 yr. Both Antevs' early studies and more recent modeling results suggest that at least the most

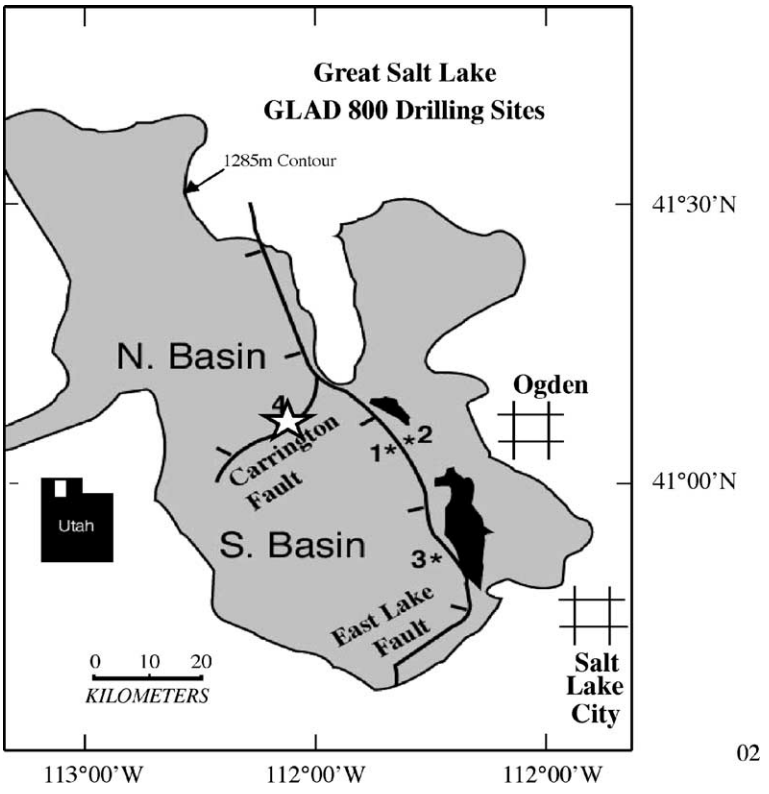

Fig. 1. Map of the Great Salt Lake. The 'star' shows the location of the drilling operation for Site 4; lat: 41°07′ 50.20″, long: 112°33′ 46.48″, water depth: 9.30 m (figure adapted from Dean et al., 2002).

recent of these lake level fluctuations (the "Lake Bonneville" phase) may have been linked to the southward migration of the jet stream during Northern Hemisphere glacial advance (Antevs, 1948; COHMAP, 1988; Thompson et al., 1993; Kutzbach et al., 1994). A southward migration of the jet stream from its current position could be expected to bring more precipitation to the eastern Great Basin and, therefore, lakes in the eastern Great Basin become deeper during the glacial advance. The late Pleistocene 'Lake Bonneville' phase has been the most intensively studied of all the deep lake cycles because of its abundant evidence from outcrops of deepwater and shoreline terrace deposits. High stands in this most recent deep lake cycle are clearly correlated with the most recent glacial advance (i.e. Scott et al., 1983; Spencer et al., 1984; Currey and Oviatt, 1985; Oviatt et al., 1992, 1999; Oviatt, 1997). However, earlier deep lake cycles also appear to be associated in time with the global oxygen isotope record. The deep lake cycle known as Cutler Dam preceded Lake Bonneville, and has been correlated with the OIS 4/OIS 3 transition (Oviatt et al., 1987; Kaufman et al., 2001). Two older deep lake cycles, the Little Valley cycle, which has been associated with glacial stage OIS 6 (Scott et al., 1983; Oviatt et al., 1999) and the Pokes Point cycle, associated with OIS 12 (Oviatt et al., 1999), are also known from outcrops but remain poorly understood. At least four lake cycles were also recognized in the Burmester core, taken from near the modern lake's shoreline, the oldest of which is slightly older than the Lava Creek B tephra from Yellowstone (~650 ka) (Oviatt et al., 1999).

Today, all that remains of Lake Bonneville is a patch of briny water, otherwise known as the Great Salt Lake. Buried deep beneath this lake is a well-preserved stratigraphic record of the Bonneville basin's climate-driven past. Wells drilled by Amoco Production in the late 1970s provided researchers with evidence that the sediments beneath the Great Salt

Lake contain one of the most continuous Neogene records of North American climate and environmental change (Davis, 1998; Davis and Moutoux, 1998; Kowalewska and Cohen, 1998). Obtaining a long, continuous core from this basin has the potential to give one of the best and most complete paleoclimate records to date and this is one of the primary reasons scientists from the University of Minnesota, University of Arizona and the USGS chose the Great Salt Lake as its first test of the GLAD 800 Drilling system.

2. Methods

We have assembled a ~2000 yr resolution paleoenvironmental record using sedimentary facies and fossil invertebrates from Site 4 as indicators of environmental and ecosystem response to climate change. A detailed sedimentary facies analysis was performed as part of the Initial Core Description following the Limnological Research Center (LRC) procedures described in detail elsewhere (Palacios et al., 2001). Cores were logged using a MultiSensor Core Logging (MSCL) including Magnetic Susceptibility, Gamma-ray Densitometry and P-wave velocity. A detailed visual core description allowed the identification of sedimentary units based on color, grain-size, sedimentary textures and structures, and fossil content. Smear slides and selected X-ray diffraction analyses permit the definition of the sedimentary facies according to the LRC component-based sediment classification (Schnurrenberger et al., 2003).

We have chosen ostracode fossils as our primary indicator because they have proven to be extremely useful in the reconstruction of lacustrine paleoenvironments, through their rapid response (in the form of changing species composition, abundance and diversity) to climate-related limnologic change. Other fossil invertebrates were also used as paleoecological indicators in this study. Both brine shrimp and brine fly fossils are excellent indicators of hypersaline environments because they have a much higher salinity tolerance than most other invertebrates. Brine shrimp (*Artemia salina*) fossils are in the form of eggs, fecal pellets and occasionally chitinous exoskeletal fragments. Brine fly larvae (*Ephydra riparia*) are abundantly preserved as highly sclerotized proleg claws, or less commonly as intact larvae, adults or exoskeletal fragments. Lastly, freshwater molluscs were used as indicators of marsh or shallow littoral environments. *Physella* spp. and various species of planorbid gastropods were found in many horizons.

Samples were taken from Site 4 at 1 m intervals to supplement the core catcher samples obtained during the August 2000 drilling operation. We disaggregated, cleaned and processed all core samples using a variant of the methods of Forester et al. (1994). Using a 125-micron sieve, we separated the ostracodes and coarser sediments from the finer material. The >125-micron fraction was oven dried at 40 °C and weighed. Micropaleontologic and sedimentary indicators were visually estimated as percent per sample using Olympus SZX12 and Leica MZ12 stereo microscopes. Micropaleontologic indicators include ostracodes, brine shrimp fossils, brine fly fossils, gastropods and bivalves. Sedimentary indicators include quartz grains, mafic and other terrigenous sediments and pyrite. Samples that contained a high abundance of ostracodes and/or brine shrimp fossils were sub-sampled and counted. The dry weights of both the subsample and the sample were used to estimate number/g. In samples that had low abundance of ostracodes all were counted, otherwise, ostracodes were counted to 300 individuals. Both juveniles and adults were counted, but only adults/sub-adults were identified and used in our paleoecological interpretations. Identification was to the lowest possible taxonomic level, usually species, and was based on published sources (Delorme, 1970a,b,c,d, 1971, 1991), personal communication with Dr. Richard Forester of the USGS and Dr. Manuel Palacios-Fest of Terra Nostra Earth Science Research and comparison with the University of Arizona lacustrine ostracode collection.

We used DCA (detrended correspondence analysis) to gain a better understanding of the spatial/temporal variability of ostracode assemblages throughout the core. This method of indirect gradient analysis arranges samples from the core containing ostracodes in multivariate space, and is ideal for the analysis of fossil assemblage data for which individual species abundance responses to environmental forcing variables are unimodal (ter Braak and Prentice, 1988; ter Braak and Smilauer, 1998). Samples that cluster together have similar species compositions and

samples that are separated in multivariate space have less similar compositions. Because explicit (i.e. modern) ostracode-environmental data were not compiled, direct gradient analysis such as CCA (Canonical Correspondence Analysis) could not be used. Therefore, the significance of multivariate axes must be inferred from our general knowledge of the distribution of these ostracode species in modern environments (see e.g. Delorme, 1970a,b,c,d, 1971, 1991; Palacios-Fest et al., 1994; Holmes and Chivas, 2002; Forester, 1983, 1985, 1986, 1987, 1991a,b; Forester and Brouwers, 1985; Smith, 1993a,b; Smith et al., 1992). To increase the robustness of our multivariate analysis, we applied the following constraints: (i) only ostracode taxa that had an abundance of 10 individuals/g in at least one sample were included and (ii) samples had to contain at least 10 ostracodes/g to be included. Ostracode percent data were arc-sin transformed prior to analysis, and analyzed using DCA with CANOCO 4 for WINDOWS (ter Braak and Smilauer, 1998). DCA plots were generated in CanoDraw and modified for clarity in Adobe Illustrator and Microsoft Powerpoint.

2.1. Geochronology and age model

A combination of new radiocarbon and U-series data, coupled with biostratigraphic and tephra correlations constrain the timing of environmental changes recorded by our paleontological and sedimentological indicators (Fig. 2). Radiocarbon dates provide age constraints for sediments younger than ~30,000 cal yr BP. ^{14}C AMS dating was only possible above the upper salt horizon, less than 9 mblf (<10,920 cal yr BP) because there was no datable terrestrial material between the evaporite layer and the maximum depth (age) allowable for reliable radiocarbon dates. Lacustrine organic material could not be used for ^{14}C dating because of unknown and likely variable reservoir effects. U-series geochronology was used to constrain the age of sediments older than 30,000 yr BP. This dating method is commonly used in studies of Quaternary climate change because it can accurately date evaporite and aragonitic deposits beyond the limit of radiocarbon dating (e.g. Lin et al., 1996). Two U-series dates were obtained from endogenic carbonate minerals for the preliminary study (Dean et al., 2002) and yielded preliminary (uncorrected for initial ^{230}Th) ages of 41,000 cal yr BP at 19 mblf and 231,000 cal yr BP at 95.6 mblf. As these dates are calculated assuming all measured ^{230}Th is radiogenic, these are robust *maximum* ages of the samples. The uppermost sample is constrained by the Hansel Valley ash at 17.2 mblf (26,500 cal yr BP, although more recent work by Oviatt (personal communication) suggests that this tephra may be closer to 24,000 cal yr BP) consistent with the maximum estimates by U/Th dates. Material for new U-series dating came from the two thick evaporite layers found from 14.34 to 10.62 mblf and from 70.63 to 67.79 mblf.

2.2. ^{14}C AMS geochronology

Nine samples within the upper 12 m contained material that could be used for radiocarbon dating. The material was primarily hand-picked charcoal, however, one sample was 150 μg of hand-picked leaf hairs (taxonomy unknown, but unquestionably from terrestrial plant families). These structures are quite delicate and are unlikely to be reworked. The charcoal samples could not be accurately weighed before pretreatment because they were extremely small (<50 μg). Samples were pretreated, combusted and processed at the AMS Laboratory at the University of Arizona. All samples were assumed to be of terrestrial origin, and therefore were not subjected to any reservoir corrections. We calibrated all radiocarbon dates to calendar years using Calib 4.4 (www.depts.washington.edu/qil/calib) and are presented $\pm 2\sigma$ in Table 1. If the radiocarbon age was beyond the range for tree ring calibration curves (only the case for previously published ^{14}C dates), we used a mean calibrated age calculated from two different calibration curves, one generated from stalagmite data and the other from Lake Suigetsu's annually laminated sediments (Beck et al., 2001; Kitagawa and van der Plicht, 1998).

2.3. U-series geochronology

Material for the U-series dates came from evaporite deposits from two core horizons; core drives 4A-6A-1 (41 cm, 11.89 mblf) and 4B-10A-1 (40 cm, 68.11 mblf). The evaporite deposits consisted of the minerals thernardite (Na_2SO_4) and halite (NaCl), respectively. The U/Th dating was performed at the

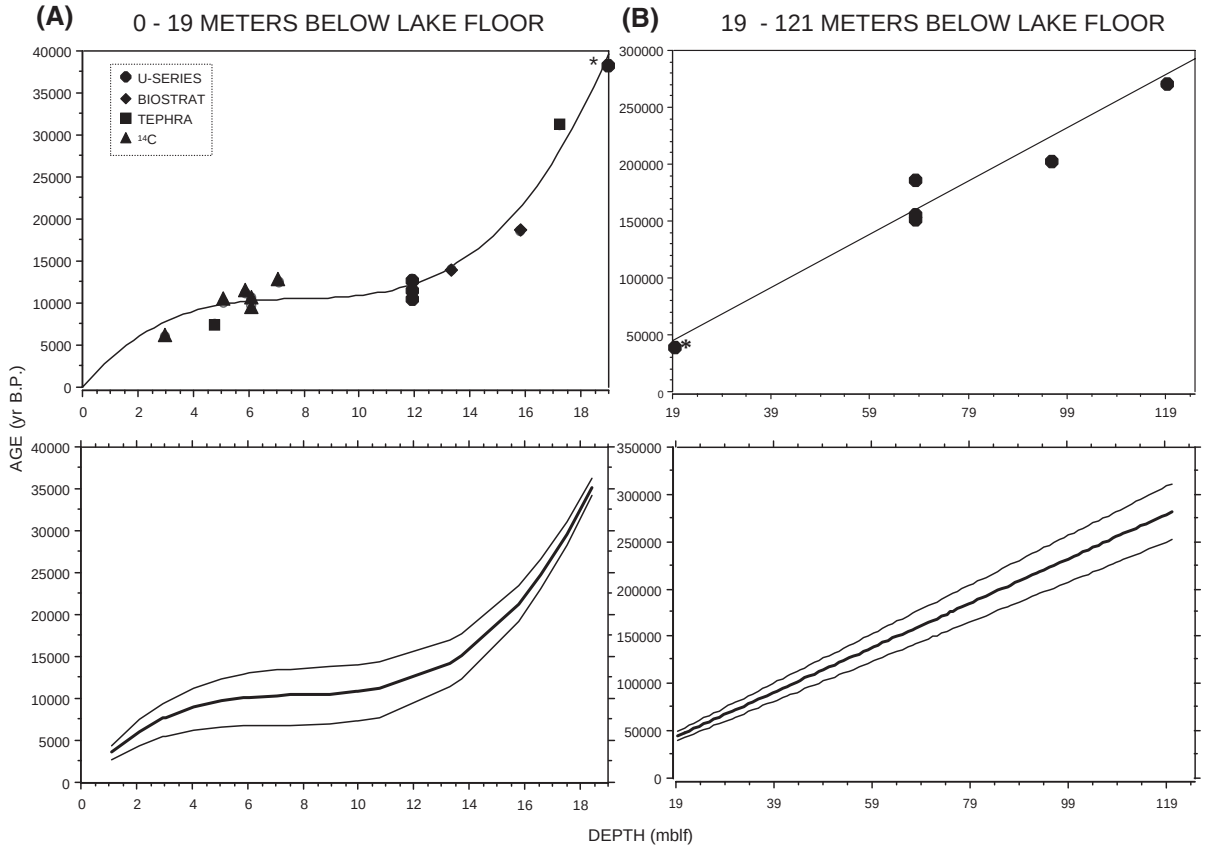

Fig. 2. Age models generated for Site 4. We calculated split regressions using a combination of ^{14}C, U-series, tephra and biostratigraphic correlation dates. (A, top) Regression for upper 19 mblf ($y=20.3x^3-478.49x^2+3845.21x$); and regression including standard error confidence interval (A, bottom: upper limit is $y=20.77x^3-523.42x^2+4570.99x$; lower limit is $y=18.93x^3-404.41x^2+2891.11x$). (B, top) Regression for 19–121 mblf ($y=2344.3x$), and regression including standard error confidence interval (B, bottom: upper limit is $y=2591.93x$; lower limit is $y=2096.61x$). (*) U–Th datapoint used to join the upper and lower regressions. The datapoint (19 mblf: 38,700±2500 was used to calculate regressions in both (A) and (B). Confidence intervals (lower left) are only shown starting from our first data point at 1 mblf.

Minnesota Isotope Laboratory, Department of Geology and Geophysics, University of Minnesota (Table 2). ~0.5 g of salt sample and ~15 mg of aragonite sample were dissolved in concentrated HNO_3 acid and then mixed with a mixed spike containing ^{229}Th, ^{233}U and ^{236}U. The aragonite was present in the core in thin (~2 mm) laminations composed of nearly pure fine-grained aragonite. The small aragonite sample-size was specifically chosen so that we could obtain relatively pure aragonite sub-samples from the core

Table 1
AMS ^{14}C dates from the upper 12 m of Site 4

AA number	Laboratory number	Sample ID	Depth (mblf)	δC^{13}	^{14}C yr	cal yr BP
AA53602	T17311	GSL-2	2.95	M	5500±740	6148±1642
AA53605	T17314	GSL-5	5.06	M	8800±1300	10,209±3005
AA53606	T17315	GSL-6	5.88	M	9600±1300	11,381±3950
AA53607	T17316	GSL-7	6.05	M	8500±1500	9873±3566
AA53608	T17317	GSL-8	6.05	M	9300±1500	10,747±3588
AA53609	T17318	GSL-9	7.05	M	10,700±1800	12,545±4400

Table 2
^{230}Th dating results

Sample number	Laboratory number	Depth (mblf)	Mineral	^{238}U (ppb)	^{232}Th (ppt)	^{230}Th/^{232}Th (atomic$\times10^{-6}$)	δ^{234}U* (measured)	^{230}Th/^{238}U (activity)	^{230}Th age (years) (uncorrected)	^{230}Th age (years) (corrected)	$\delta^{234}U_{Initial}$** (corrected)
GSL004A-6A	A1	11.89	thernardite	1.64±0.01	1124±5	6.5±0.4	1023±16	0.271±0.017	15,550±1050	11,070±4700	1038±23
	A2	11.89	thernardite	2.00±0.01	1400±5	7.2±0.3	1039±14	0.305±0.014	17,470±890	12,940±4700	1061±22
	A3	11.89	thernardite	1.82±0.01	1293±5	6.8±0.4	1034±15	0.291±0.017	16,650±1000	12,020±4800	1052±22
	MC-01	19.00	aragonite	5640±10	2,278,850±60,800	27.1±0.7	1052±3	0.6636±0.0032	41,200±240	38,700±2500	1174±9
GSL004B10A	B1	68.11	halite	1.52±0.01	2821±10	13.7±0.4	675±24	1.534±0.043	197,700±15,500	186,000±19,000	1141±75
	B2	68.11	halite	1.50±0.01	2368±9	14.1±0.4	616±22	1.354±0.039	164,200±11,000	153,000±16,000	950±55
	B3	68.11	halite	1.31±0.02	2066±22	16.0±0.9	667±115	1.522±0.083	197,000±50,000	187,000±44,000	1130±250
	B4	68.11	halite	1.18±0.01	2012±10	14.0±0.5	691±44	1.446±0.052	170,000±16,800	158,000±19,000	1080±90
	BB	95.60	aragonite	3768±16	6,457,500±152,500	13.9±0.5	512±9	1.448±0.036	231,000±17,000	202,000±19,000	904±51
	AA	118.70	aragonite	3822±8	4,323,700±111,300	23.0±0.7	534±8	1.574±0.021	287,000±15,500	271,000±16,000	1147±52

All errors are 2σ. We used the following values for decay constants in our age calculations: λ_{230}=9.1577×10^{-6} yr^{-1}, λ_{234}=2.8263×10^{-6} yr^{-1}, λ_{238}=1.55125×10^{-10} yr^{-1} (see Cheng et al., 2000a,b). *$\delta^{234}U=([^{234}U/^{238}U]_{activity}-1)\times1000$. **$\delta^{234}U_{initial}$ was calculated based on ^{230}Th age (T), i.e., $\delta^{234}U_{initial}=\delta^{234}U_{measured}\times e^{\lambda 234xT}$. Corrected ^{230}Th ages are based on an initial ^{230}Th/^{232}Th atomic ratio of 2±2×10^{-6}, a value which places sample GSL004A-6A in the stratigraphic order constrained by our ^{14}C dating (upper limit, ~8000 cal yr BP) and a biostratigraphic correlation (lower limit, 14,400 cal yr BP) (Table 3).

and thereby minimize errors associated with correction for initial ^{230}Th. Although the small sample size increases the analytical error in the measurement of the uranium-series nuclides, it decreases the overall error, as error associated with correction for initial ^{230}Th is reduced. U and Th chemical separation procedures are outlined in Edwards et al. (1987). After the purification U and Th fractions were dissolved in 1% HNO_3 for analysis by magnetic sector inductively coupled plasma mass spectrometry (ICP-MS, Thermo-Finnigan MAT Element I), following procedures described in Cheng et al. (2000a,b) and Shen et al. (2002). Isochron methods were not used to correct for initial ^{230}Th as the range in ^{232}Th/^{238}U was inadequate. Instead, we determined strict limits on the range of possible initial ^{230}Th/^{232}Th values for three Holocene/late Pleistocene samples as follows. Maximum initial ^{230}Th/^{232}Th values were determined from the knowledge that the age of all three samples was greater than the well-constrained age of the overlying Mazama tephra (Zdanowicz et al., 1999). The maximum ^{230}Th/^{232}Th values for all three samples agreed within analytical error and averaged 3.3×10^{-6} by atom. The theoretical lower limit on initial ^{230}Th/^{232}Th is zero. We therefore applied a correction for initial ^{230}Th using an initial ^{230}Th/^{232}Th value of 2±2×10^{-6}. Including the error, this correction covers the full range of initial ^{230}Th/^{232}Th values from the theoretical lower limit of zero, to values significantly greater than our observed maximum values. The method that we used to constrain initial ^{230}Th/^{232}Th values is not as well known as the isochron method; however, in the right circumstances can be equally powerful. More extensive discussion and other applications of the principles applied here can be found in Cheng et al. (2000a,b) and Cobb et al. (2003).We applied this correction to all U/Th dates and used these corrected values for our age model. Use of this correction required the assumption that initial ^{230}Th/^{232}Th values did not changed with time, beyond the range allowed by our error bars. At the lower end of the range, this assumption must be true as the lowest initial ^{230}Th/^{232}Th in our range is zero, the theoretical lower limit. At the upper end of the range, we cannot definitively rule out the possibility that initial ^{230}Th/^{232}Th values could have exceeded the maximum value accommodated by our correction

(4×10^{-6}). On the other hand, we have no evidence that initial $^{230}Th/^{232}Th$ values did exceed these values. Furthermore, corrections for initial ^{230}Th for the samples beyond the radiocarbon range (where are chronology relies most strongly on the U/Th ages) were relatively small. Finally, in conjunction with other age data, the corrected ages yielded a self-consistent age model as there is only a small gap in age estimates between the two regressions, and the corrected ages agree well with age estimates from other sources. Our confidence in the U-series age estimates is strengthened by the fact that the resulting age model produces age picks for deep water deposits that are consistent with pre-existing age constraints for two previously recognized Pleistocene high-stand lake cycles. These horizons (correlative with the Little Valley and Cutler Dam Highstands) were intentionally left out of our age modeling data, and therefore provide an independent check on the accuracy of the U-series-based chronology prior to the late Pleistocene.

2.4. Tephra and biostratigraphic correlation

Two tephra layers have been positively identified in the core. The Mazama ash is located 4.77 mblf and has a published age of 7627±150 cal yr BP, which is very well constrained (Zdanowicz et al., 1999). The Hansel Valley Ash appears 17.2 mblf and has a published age of 31,288±127 cal yr BP (Oviatt et al., 1992), although, as noted earlier, Oviatt (personal communication) suggests that this date may be too old by several thousand years.

We used biostratigraphic correlations for two age constraints on horizons 13.31 and 15.79 mblf. Our correlation at 15.79 mblf used an assemblage containing the ostracode species *Candona aduncа* and *Limnocythere ceriotuberosa*, an assemblage that has, to date, only been associated with the middle transgressive phase of Lake Bonneville, dated in other deposits at between 21,000 and 14,600 cal yr BP (19,000–14,000 ^{14}C yr BP (Thompson et al., 1990; Oviatt et al., 1992, Oviatt, personal communication, 2004). Our other age constraints suggest that the 15.79 m sample lies near the older end of this range and for the purpose of developing an age model we have used the published date of 18,718±290 cal yr BP (15,860±180 ^{14}C yr BP) for the horizon containing this assemblage (Thompson et al., 1990, Oviatt et al., 1992). A sample at 16.59 m containing *Limnocythere staplini* and *Candona caudata* is probably correlative with an algal-laminated "Stansbury" lake stand interval in the range of ~21,400–26,000 cal yr BP (20–22,000 ^{14}C yr BP) (Oviatt et al., 1990, and personal communication, 2004).

At 13.31 mblf, above the Bonneville highstand deposits, the only invertebrate fossils present in our core sample are brine shrimp eggs. This is consistent with other shoreline and core evidence, which indicates that after the Bonneville highstand, eggs appear in the fossil record before brine shrimp pellets (Oviatt, personal communication, 2003). We correlated our brine shrimp eggs with the middle of unit IIIa in the core studied by Thompson et al. (1990). The middle of unit IIIa was deposited above the indicators of the Bonneville highstand and is right below the appearance of brine shrimp pellets at 14,091±283 cal yr BP (12,100±130 ^{14}C yr BP).

Our age model uses a combination of dates generated by ^{14}C and U-series dating, plus the constraints provided by the tephra and biostratigraphic correlations discussed above (see Table 3). Because the dated material is not evenly dispersed throughout the core, we generated our age model using a split-regression (Fig. 2). We used a non-linear, third order polynomial regression for mean age estimates in the upper portion of the core (<19 mblf). This provided age estimates that were most consistent with the well-constrained Mazama and moderately constrained Hansel Valley tephra dates, and is consistent with: (*i*) expected faster sedimentation rates during the Pleistocene/Holocene boundary evaporite deposition and (*ii*) slower sedimentation rates in the less compacted core top sediments. The age model for the bottom part of the core was generated with a linear regression because the dates in the lower portion of the core are less constrained than the upper part of the core. Also, linear regression, as opposed to non-linear regression, reduced the gap between the split regressions, allowing a more continuous estimate of ages.

We calculated the expected *mean* age for a given depth by generating the regression equations discussed above with 'depth' as our independent variable and 'mean date' as our dependent variable. To calculate the expected *range* of ages for a given

Table 3
Dates used to generate age model

Depth (mblf)	Method	Dates (U-series uncorrected)	Dates (U-series corrected)	Reference
2.95	carbon14 (charcoal)	6148±1642 cal yr BP	6148±1642 cal yr BP	this paper
4.77	tephra correlation (Mazama)	7627±150 cal yr BP	7627±150 cal yr BP	Zdanowicz et al., 1999
5.06	carbon14 (charcoal)	10,209±3005 cal yr BP	10,209±3005 cal yr BP	this paper
5.88	carbon14 (charcoal)	11,381±3950 cal yr BP	11,381±3950 cal yr BP	this paper
6.05	carbon14 (charcoal)	9873±3566 cal yr BP	9873±3566 cal yr BP	this paper
6.05	carbon14 (leaf hairs)	10,747±3588 cal yr BP	10,747±3588 cal yr BP	this paper
7.05	carbon14 (charcoal)	12,545±4400 cal yr BP	12,545±4400 cal yr BP	this paper
11.89	U-series	15,550±1050 yr BP	11,070±4700 yr BP	this paper
11.89	U-series	17,470±890 yr BP	12,940±4700 yr BP	this paper
11.89	U-series	16,650±1000 yr BP	12,020±4800 yr BP	this paper
13.31	biostratigraphic correlation	14,091±283 cal yr BP	14,091±283 cal yr BP	Thompson et al., 1990
15.79	biostratigraphic correlation	18,718±290 cal yr BP	18,718±290 cal yr BP	Thompson et al., 1990
17.20	tephra correlation (Hansel Valley)	31,288±127 cal yr BP	31,288±127 cal yr BP	Oviatt et al., 1992
19.00	U-series	41,200±240 yr BP	38,700±2500 yr BP	this paper
68.11	U-series	197,700±15,500 yr BP	186,000±19,000 yr BP	this paper
68.11	U-series	164,200±11,000 yr BP	153,000±16,000 yr BP	this paper
68.11	U-series	197,000±50,000 yr BP	187,000±44,000 yr BP	this paper
68.11	U-series	170,000±16,800 yr BP	158,000±19,000 yr BP	this paper
95.60	U-series	231,000±17,000 yr BP	202,000±19,000 yr BP	this paper
118.70	U-series	287,000±15,500 yr BP	271,000±16,000 yr BP	this paper

depth, we used the upper and lower data points for each date (i.e. by adding and subtracting the standard error, respectively) as the dependent variables in the regression equations. The lower data points were used to calculate our lower confidence limit and the upper data points were used to calculate our upper confidence limit. Because of inherent uncertainty in the age estimates we present all values rounded to two significant digits. We emphasize that the age model and event chronology we present here is dependent on the accuracy of the absolute age constraints available to us: both the model and assigned absolute ages of events would likely be refined with future improvements in age-dating of the core.

3. Results

3.1. Sedimentary facies

Large changes in paleohydrological conditions and depositional environments at Site 4 are indicated by the occurrence of a variety of sedimentary facies (Fig. 3, and see Palacios et al., 2001). The bottom 4 m of Site 4 is composed of alternating decimeter-thick layers of: 1) variegated, finely laminated carbonate muds and 2) laminated (>1 cm) gray carbonate muds. Finely laminated and variegated carbonate mud are common facies in brackish to saline lake depositional environments (Renaut and Last, 1994). The occurrence of laminated, diatomaceous and carbonate muds at the bottom of the hole suggest open, saline lacustrine environments. From 117 to 105 mblf massive, silty carbonate, and gastropod-rich muds and greenish gray sandy facies with brown horizons (paleosols) reflect low, fluctuating water levels, higher clastic input (also evident in the magnetic susceptibility record) and marshy environments. Our microsedimentological core samples indicate abundant pyrite in this unit along with fluxes of quartz grains. Above this, from 105 to 98 m, soil-structures (brown-colored intervals, cracks and intense mottling) are more frequent in the massive, disturbed, gastropod-rich, pale green carbonate muds. From 98 to 85 mblf there are intervals of banded, centimeter-bedded, or finely laminated dark gray (with some dolomite), green or gray carbonate muds, and massive to poorly bedded sands. Quartz grains are abundant in the sandy intervals but there is no pyrite. The absence of soil features and subaerial exposure structures indicates a deeper depositional environment than in the 117–98 mblf interval; the presence of sandy intervals, however, suggests littoral–deltaic subenvironments associated with the saline lake subenvironments. From 85

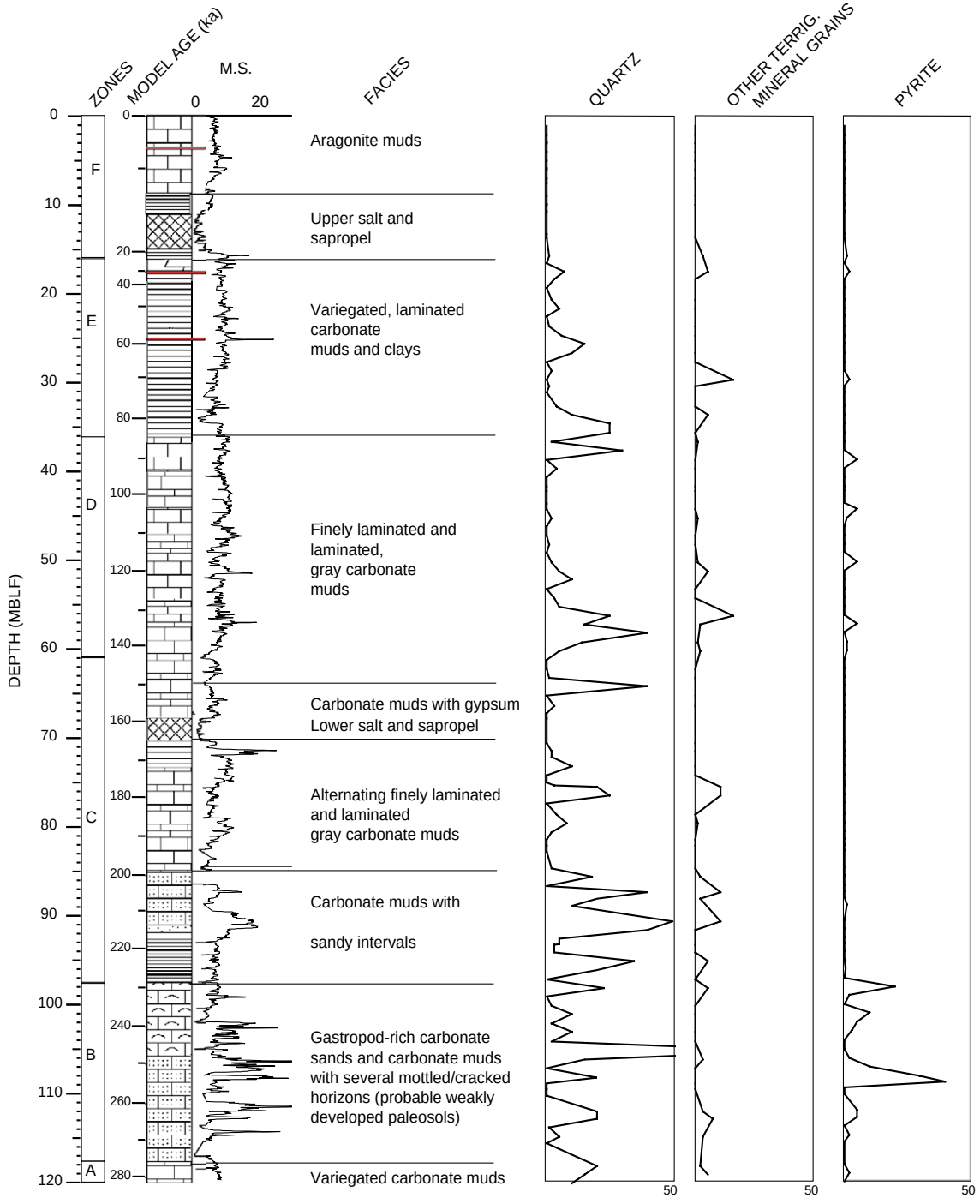

Fig. 3. Lithostratigraphy and zonation of Site 4. Zonation corresponds to the zones discussed in the text.

to 71 mblf we observe finely laminated carbonate muds and some clays. Some of the muddy horizons contain dolomite and diatomaceous muds. Sandy intervals are absent. The finely laminated and variegated nature of these facies and the absence of sandy intervals suggest offshore, deeper and brackish to saline depositional environments. A transition to more saline environments is marked towards the top of the unit by the occurrence of intercalated gypsum crystals.

The first of two evaporite layers appears from 71 to 67 mblf. The main chemical composition of this massive lower salt crust is halite (NaCl) with some carbonate mud laminae intercalated. Above the evaporite, from 67 to 65 mblf, are gray/green carbonate muds containing gypsum in centimeter-thick layers. From 65 to 36 mblf finely laminated, laminated, and massive gray carbonate muds and silts alternate. Between 63 and 61.5 mblf sediments are composed of alternating millimeter-laminated, centimeter-laminated and massive layers of gray carbonate muds. From 61.5 to 57 mblf laminated light and dark gray muds with some sandy lenses and reddish, algal-rich laminae occur. Dark gray muds occur in layers up to 1 cm thick; light gray layers are up to 2 cm thick. From 57 to 55 mblf sediments are characterized by the presence of massive to banded gray silty carbonate muds arranged in decimeter-thick fining upward sequences with subaerial exposure features at the top. Some reddish, algal-rich laminae occur. Terrigenous sediment grains, including quartz grains, are abundant, peaking around 56 mblf, in massive-banded gray silty carbonate muds with subaerial exposure features. From 54 to 36 mblf, two facies associations occur: 1) finely laminated, variegated carbonate muds and/or clays, dominant between 54 and 52 and between 44 and 40 mblf, and 2) mottled carbonate muds with dewatering structures, roots, soft sediment deformation and pseudomicrokarst structures, dominant in the remainder of the interval. The lithology changes above 36 mblf to finely laminated variegated (gray, green and black) carbonate muds and clays, with some sandy and algal rich (diatomaceous) layers. The Hansel Valley ash is located at 17.20 mblf, within massive to finely laminated black diatomaceous clays that grade upcore into carbonate (dolomite and aragonite) massive to banded muds. One meter of black sapropelic muds above ~15.6 mblf is directly overlain by a 3 m thick salt crust. This salt crust is mainly thenardite (Na_2SO_4) with massive to millimeter-interbeds of black sapropelic mud. The salt is overlain by black sapropel carbonate muds containing salt crystals (11–8.2 mblf), which grades into the top unit (8.20–0 mblf) composed of pelleted banded, aragonite muds.

3.2. Biofacies

The distribution of Site 4 biofacies are shown in Fig. 4. The bottom of the core, 121 mblf, contains abundant brine shrimp fecal pellets and a monospecific ostracode assemblage of *Limnocythere staplini*, an ostracode that requires water with a low alkalinity/Ca ratio, and which can tolerate high salinity conditions. Above 119 mblf, *L. staplini* disappears but brine shrimp pellets persist along with the occurrence of brine fly fossils. Between 115 and 113 mblf, there are few/no fossils. *L. staplini* reoccurs at 113 mblf and brine shrimp eggs make their first occurrence within the same horizon. *L. staplini* dominates very small yet diverse communities of ostracodes from 113 to 108 mblf, with certain horizons containing molluscs. Brine shrimp fossils are also present throughout this interval but are extremely scarce. Other ostracode species present in this interval include *Candona patzcuaro* (a halolerant species), *Limnocythere friabilis* and *Limnocythere ceriotuberosa*. *L. ceriotuberosa* typically becomes more abundant in conditions of somewhat higher alkalinity/Ca ratios than those favored by *L. staplini*. Increasing alkalinity/Ca ratios in this lake system are typical of increased river input, consistent with evidence for deltaic progradation onto the core site at this stratigraphic level discussed earlier. Diversity reaches its maximum in this interval at 112 mblf, with an assemblage that includes the aforementioned species and also *Limnocythere itasca*, *Cyprideis salebrosa* and *Candona caudata*. Species diversity decreases above this horizon, but ostracode carapaces become more abundant from 107 to 105 mblf with assemblages dominated by *L. staplini*, *C. patzcuaro* and *Cyprideis beaconensis*. *Cyprideis* species are typically estuarine ostracodes, but often become established in marshy areas around lake margins. Many of the ostracode carapaces are reduction stained. Molluscs and diatoms are also abundant in

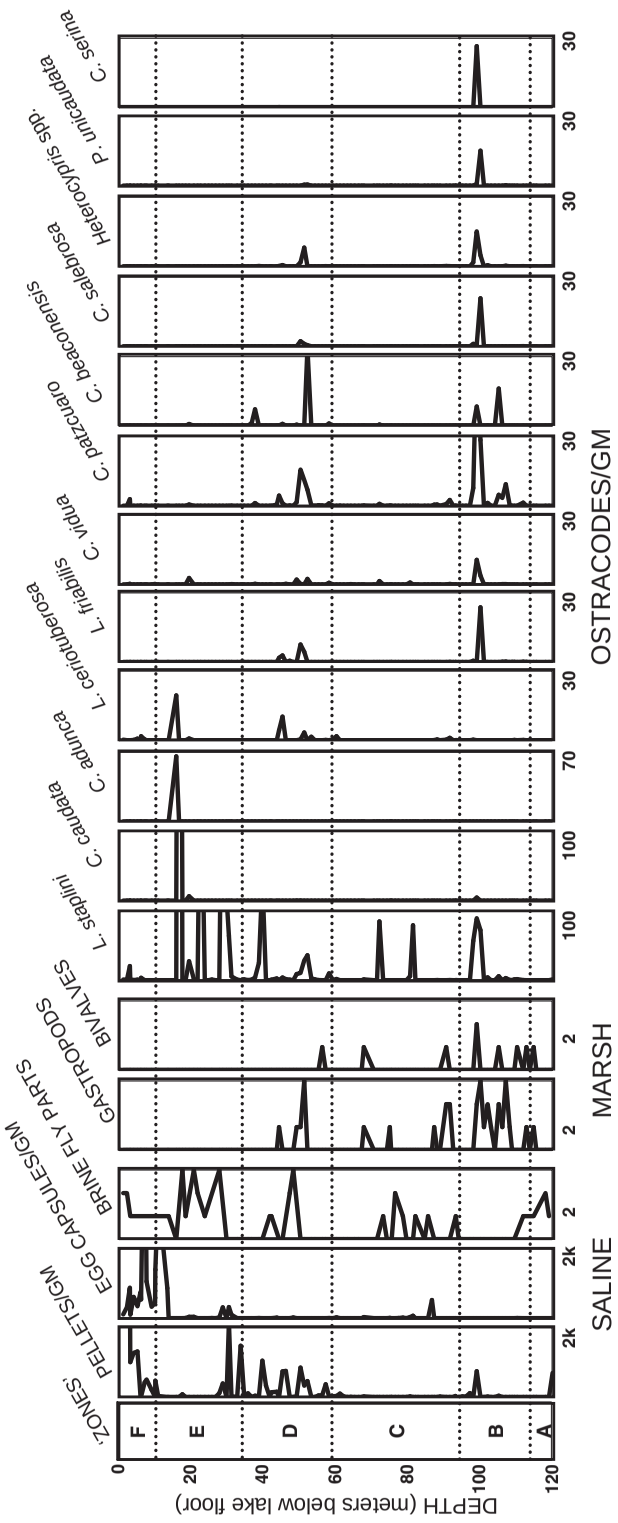

Fig. 4. Paleoecology and zonation of Site 4. We quantified brine shrimp pellets, eggs and ostracodes as number/g sediment. We measured the quantity of brine fly parts, gastropods, bivalves and fish bones on a ratio scale of absent (0), present (1) and abundant (2).

this interval and in one horizon, ~106 mblf, we found sponge spicules and fossilized sponge tissue. Ostracode carapaces, particularly *L. staplini* are found from 103 to 100 mblf along with a few brine shrimp pellets. Ostracodes are found in high abundance from 100 to 98 mblf, with highly diverse assemblages including species such as *L. staplini*, *C. patzcuaro*, *C. salebrosa*, *Cyclocypris* cf. *serina*, *Hetercypris* spp. and *Cypridopsis vidua*. Many of the carapaces are reduction stained and molluscs, particularly gastropods, are also abundant. Above 97 mblf, all ostracodes and molluscs disappear. From 97 to 92 mblf, brine shrimp fossils increase in frequency but remain relatively rare. Ostracodes are rare but diverse from 93 to 87 mblf with *L. ceriotuberosa*, *L. itasca*, *L. staplini* and *C. patzcuaro* as the dominant species. Gastropods appear once again in a thin, sandy interval from 91 to 90 mblf. *L. staplini*-dominated assemblages are found sporadically from 87 to 53 mblf, but in most intervals we found no fossils or only brine shrimp/brine fly fossils at these depths. There are only three horizons in this interval (~81, 72 and 58 mblf) where ostracodes are very abundant. In each of these cases, the ostracode assemblages are strongly dominated by *L. staplini*. At 71.5 mblf, the only ostracodes present in the core are two adult *Candona* spp. individuals in good/fair taphonomic condition, indicative of freshwater conditions. From 52 to 49 mblf, ostracodes are highly abundant and diverse. This assemblage includes *L. staplini*, *C. beaconensis*, *C. patzcuaro*, *Heterocypris* spp. (common marsh species), *C. vidua* (typical of groundwater-fed wetlands), *L. friabilis* and *L. ceriotuberosa*. Molluscs are also abundant in this interval. From 49 to 45 mblf, ostracodes remain in the fossil record but decrease in both abundance and diversity. An assemblage of abundant ostracodes, dominated by *Limnocythere platyforma* (freshwater ecophenotype of *L. ceriotuberosa*) and *L. friabilis*, is present in a thin interval around 45 mblf. From 45 to 17 mblf there are no or few ostracodes, except for isolated horizons (39–37 mblf, 30–28 mblf, 22.6 mblf and 19.4 mblf) where *L. staplini* is dominant and highly abundant. At 16.59 mblf, we find an assemblage of *L. staplini* and *C.* (cf.) *caudata*. Ostracodes are very abundant in this horizon. Directly above this, at 15.79 mblf, we found abundant *Candona adunca* and *L. ceriotuberosa*, indicative of freshwater conditions. No in situ ostracodes were found in or above the upper salt crust. Ostracode carapaces are present at these depths but they are in poor taphonomic condition (i.e. coated and broken), and believed to be reworked. Within an interval of evaporite deposition, at 13.31 mblf, brine shrimp eggs occur, overlain by brine fly fossils and abundant brine shrimp fecal pellets.

3.3. Multivariate analysis

Fig. 5 presents the DCA results for the ostracode species and samples that qualified for the multivariate analysis. DCA major axes 1 and 2 account for 28.3% and 16.7% of the total variance, respectively. DCA plots for species and samples suggest that Axis 1 represents a salinity gradient (i.e., more negative values corresponding to fresher water conditions) and Axis 2 may represent a vegetation or lake level gradient (i.e., more positive values as conditions trend towards extensive marsh vegetation, typical of lower lake levels, and more negative values when lake levels rose and the core site was transformed into an open-water lake environment). However a more robust analysis that includes environmental data is needed. The ordination plot shows three fairly distinct assemblages: (A) salt, freshwater or groundwater-discharge marsh indicators, dominated by a high diversity of ostracodes including *Cyprideis beaconensis*, *Cyprideis salebrosa*, *Candona patzcuaro*, *Cypridopsis vidua*, *Heterocypris* spp., *Potamocypris unicaudata*, *Cyclocypris* spp, *Limnocythere ceriotuberosa* and *Limnocythere friabilis*. The last two species are probably more indicative of freshwater marsh conditions, whereas the marsh assemblages with higher proportions of *Cyprideis* species and *C. vidua* are probably indicative of more saline conditions associated with groundwater discharge; (B) shallow-offshore saline indicators, dominated by *Limnocythere staplini* (especially where *L. staplini* occurs in monospecific assemblages); (C) deep offshore freshwater indicators, dominated by freshwater species *Candona caudata* or *Candona adunca*. Arrows between these assemblages show typical transformation pathways over time. The lowest ostracode record in the core that qualified for the multivariate analysis was found at 107.21 mblf, plotted in multivariate space in group A or ‘marsh’ assemblage. Indications of an environmental shift

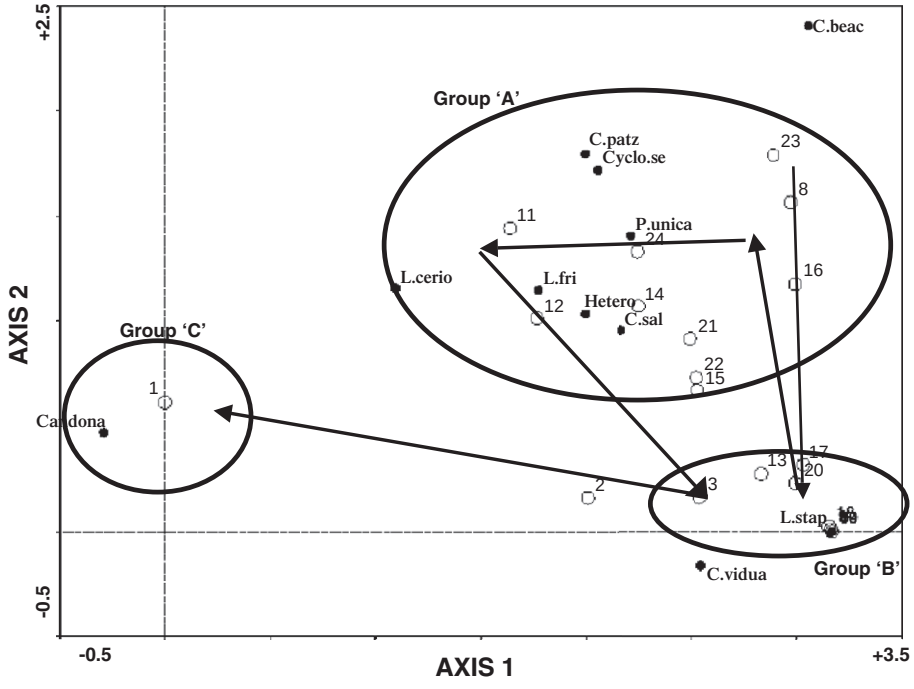

Fig. 5. Ordination plot from our multivariate analysis of the ostracode data. Group 'A' suggests 'saline/freshwater marsh' environment; Group 'B' suggests 'shallow/offshore saline' conditions and Group 'C' suggests 'deep offshore freshwater' conditions. The arrows indicate typical transformation pathways between ostracode assemblages as environments shifted through time (see text for details).

occur at 99 mblf from Group A 'marsh' to Group B 'shallow offshore saline' conditions (see arrows in Fig. 5). The saline open-water assemblage (Group B) disappears around 58 mblf. Another transition in assemblage, and hence environment, is present at 52.20 mblf where a saline marsh assemblage (Group A) becomes dominant. A slight transition within Group A occurs at 45 mblf from salt marsh indicators to freshwater marsh indicators. Shallow offshore saline conditions are present around 44 mblf where Group B becomes dominant again. Shallow offshore saline indicators prevail up to the occurrence of a thin indicator of a deep offshore freshwater event at ~16 mblf (Group C).

Our DCA analysis shows that transitions in multivariate space were most commonly between Group A, the 'marsh indicators', and Group B, the 'shallow-offshore saline indicators', whereas Group C, the 'offshore freshwater indicators', appear infrequently (see arrows in Fig. 6). This suggests that the environment at the core site has fluctuated mostly between shallow saline water and marsh conditions, with open, freshwater events extremely rare.

3.4. Biofacies and sedimentary facies zonation and paleoenvironmental interpretation

We have combined similar and contiguous lithofacies and biofacies, as well as the results of our ostracode multivariate analysis into a series of stratigraphic 'zones' (see Figs. 3–5). These zones are represented by a particular depth interval and a "best-estimate" age based on our available core geochronology (Fig. 2; note: age estimates are rounded to two significant digits from age model results). The zones elucidate the systematic environmental changes that have occurred at Site 4 over the last ~280,000 yr BP.

3.5. Zone A: 121–112 mblf (~280,000–260,000 yr BP)

Our record begins with indications of a shallow saline lake, suggested by its gray and variegated muds with fine laminations and the presence of *Limnocy-*

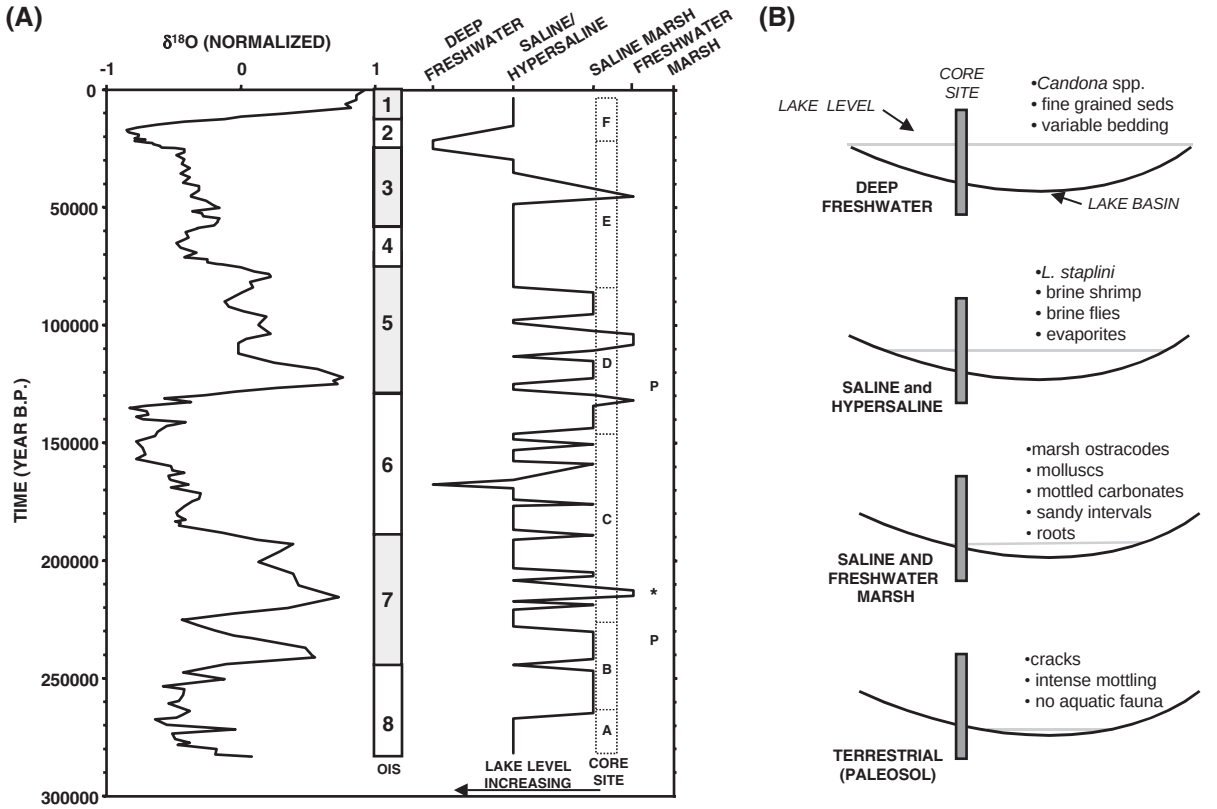

Fig. 6. (A) Comparison of Site 4 zonation and lake level oscillation with SPECMAP (from Martinson et al., 1987). An asterisk (*) indicates shallow depth may be due to delta progradation; 'P' indicates depth where paleosol deposits may occur but were not sampled. 'Core Site' designates the position of the core in relation to lake level (i.e., when lake level is deeper than the core's position, the curve is to the left of "Core Site" and when lake level is shallower than the core's position, the curve is to the right of "Core Site". "Core Site" is divided into the biofacies and sedimentary facies zonation described in the text (Zone A: 121–112 mblf, Zone B: 112–98 mblf, Zone C: 97–61 mblf, Zone D: 61–36 mblf, Zone E: 36–15.8 mblf and Zone F: 15.8–0 mblf); (B) cartoon showing core site in terms of regional lake level fluctuations. See text for discussion.

there staplini (in low abundance), brine flies and brine shrimp. Fine laminations suggest slow depositional rates and an absence of bioturbation, which are common in calm, deeper water. *L. staplini* disappear above 119 mblf (280,000±30,000 yr BP) and only brine fly and brine shrimp fossils remain. The disappearance of *L. staplini* may indicate a switch from saline to hypersaline conditions since brine flies and brine shrimp have a much higher salinity tolerance than *L. staplini*. At the top of zone A (112 mblf: 260,000±30,000 yr BP), the lithology remains the same; however, rare *L. staplini* appear, along with a small number of *Limnocythere friabilis* and molluscs. The appearance of this biological community suggests water salinity was decreasing over this time period.

3.6. Zone B: 112–98 mblf (~260,000–230,000 yr BP)

During this time period, the core site was situated on the margin of a shallow lake where the water level oscillated frequently. Brine shrimp fecal pellets are found sporadically throughout zone B but they are never abundant. Reduction stains on some pellets and ostracode carapaces are indicative of the reducing environment of marsh muds. Ostracode DCA analysis clusters samples from this zone in the 'marsh' assemblage. A high diversity of ostracodes and molluscs common to lake littoral zones are found in several intervals between 107 and 98 mblf (250,000± 30,000 to 230,000±20,000 yr BP). In particular, the presence of *Cyprideis* species and *Cypridopsis vidua*

in many of the horizons indicates a marsh hydrology occasionally dominated by groundwater discharge. Accompanying the molluscs and marsh ostracodes, we found abundant diatoms from 106 to 103 mblf (250,000±30,000 to 240,000±30,000 yr BP) and *Chara*-stems, sponge spicules and fossilized sponge tissue at 106 mblf (250,000±30,000 yr BP).

Further evidence that zone B was dominated by marsh conditions comes from the facies associations. Pyrite is common in zone B and is typically formed under reducing conditions in marsh muds. The presence of mottled, and sometimes bioturbated, muds and sandy intervals indicate a higher energy level similar to the one found along lake shorelines; as opposed to the calmer and deeper water of a lake's profundal zone. We believe water level dropped below the core site occasionally as suggested by sedimentological textures and structures such as brown-colored intervals with cracks and intense mottling indicative of soil formation.

3.7. Zone C: 98–61 mblf (~230,000–140,000 yr BP)

This zone comprises the transition from littoral, deltaic-influenced environments to saline and hypersaline off-shore lake environments. Most of this zone is indicative of saline to hypersaline, open lake conditions, based on the finely laminated muds and abundant brine fly fossils. Ostracodes are sparse in zone C, except 81 mblf (190,000±20,000 yr BP) and 72 mblf (170,000±20,000 yr BP), which contain abundant *Limnocythere staplini*, suggesting saline rather than hypersaline conditions. Because *L. staplini* is so abundant in these horizons, the ostracode DCA analysis clustered samples from this zone in the 'shallow-offshore saline' assemblage, even though we have evidence for other environments during this time period. For instance, between 91 and 90 mblf (220,000–210,000±20,000 yr BP) there are carbonate muds with chevron laminations and crossbedding topped by massive to poorly laminated quartz silty sand. Both the mud and sand contain molluscs, freshwater marsh ostracodes are present but in relatively low quantities (no *L. staplini*) and no brine fly fossils. The sample directly below this interval (92 mblf; 220,000±20,000 yr BP) contains a large amount of quartz sand and evidence of terrestrial plant and insect parts, which may suggest delta progradation at the core site. If so then the indications of a freshwater marsh environment between 91 and 90 mblf (220,000–210,000±20,000 yr BP) were not caused by decreasing lake levels but rather as a result of delta progradation out to the core site. At 88–87 mblf (210,000–200,000±20,000 yr BP) greenish gray chevron-laminated muds with crossbedding and dolomite muds with sandy silt and organic matter is found, along with a relatively low abundance of marsh ostracodes. This interval represents a short period when lake level regressed and the core site was, once again, in a marsh-type environment. Evidence of a major and rapid transgression to deeper, freshwater is found around 71.5 mblf (170,000±20,000 yr BP) with the presence, in situ, of the freshwater ostracode *Candona caudata* within finely laminated variegated muds. This may indicate a brief period of open freshwater conditions at the core site.

From 70 to 62 mblf (170,000±20,000 to 150,000±20,000 yr BP) we find evidence of highly evaporative lake conditions. The lower authigenic evaporite unit, 70.6–67.8 mblf (170,000±20,000 to 160,000±20,000 yr BP), was deposited directly above the aforementioned indications of relatively freshwater lake conditions (71.5 mblf: 170,000±20,000 yr BP). This sequence indicates rapid concentration of the lake's dissolved solutes and a hypersaline lake that reached the halite precipitation point. Sedimentological and biological indicators suggest the decline in lake level continued after deposition of the salt. Massive to banded gray and greenish gray carbonate muds with gypsum layers overlie the salt crust. A sample from the very top of the salt crust (67.8 mblf: 170,000±20,000 yr BP) contains carbonate clay–silt mud and gypsum crystals with a few brine shrimp fossils and a very low abundance of marsh ostracodes and mollusks.

3.8. Zone D: 61–36 mblf (~140,000–86,000 yr BP)

Zone D is indicative of dominantly littoral lake environments, with evidence for frequent oscillations in water level at the core site. Between 61 and 54 mblf (140,000±20,000 to 130,000±10,000 yr BP) laminated muds with sandy intervals suggest small oscillations in lake level, with the laminated muds having been deposited in calmer, deeper water and

sandy intervals coming from higher energy shoreline environments. Ostracodes occur in low abundance in this interval, except for a thin unit ~58 mblf (140,000±10,000 yr BP) where abundant *Limnocythere staplini* appear. Two meters of gray carbonate mud arranged in decimeter-thick fining upward sequences (57–55 mblf: ~130,000±10,000 yr BP) shows subaerial exposure features at the top and suggests a regressive lake phase with possible soil formation at the core site. Deposited above this, at ~54 mblf (130,000±10,000 yr BP) are laminated muds with sandy layers and no mottling, which may signal a time when lake level rose and the core site was submerged again. From 53 to 36 mblf (120,000±10,000 to 86,000±9,000 yr BP) facies indicators show that the core site was predominantly situated in a marsh-like environment with the lake level lying slightly below the core site, as suggested by the presence of marsh ostracodes, molluscs and mottled carbonate muds containing roots, dewatering structures and soft sediment deformation features. The presence of *Cyprideis* species and *Cypridopsis vidua* in some horizons indicate the marsh may have occasionally been inundated with groundwater discharge. One horizon, 45–44 mblf (~110,000–100,000±10,000 yr BP), may suggest groundwater discharge runoff maintained the marsh environment given the presence of two ostracode species, *Limnocythere friabilis* and *Limnocythere platyforma* (a freshwater ecophenotype of *Limnocythere ceriotuberosa*), both preferring cooler and fresher water. Although the lithofacies and biofacies from 53 to 36 mblf indicate predominantly marsh conditions with lake level slightly below the core site, two intervals (48–47 mblf: 110,000±10,000 yr BP and 43–40 mblf: 100,000±10,000 to 95,000± 10,000 yr BP) suggest the core site was periodically inundated by hypersaline lake water. These intervals contain no/very few ostracodes, abundant brine shrimp and brine fly fossils in finely laminated variegated muds.

3.9. Zone E: 36–15.8 mblf (~84,000–19,000 cal yr BP)

Much of zone E shows evidence of an open-saline lake as indicated by the combined presence of finely laminated gray/variegated muds and mono-specific assemblages of *Limnocythere staplini* and brine shrimp/brine fly fossils. *L. staplini* usually is present in low numbers but is abundant between 30 and 28 mblf (71,000±8000 to 67,000±7000 yr BP) and at ~22 mblf (53,000±6000 yr BP). One assemblage in zone E, ~19 mblf (45,000±5000 cal yr BP), is dominated by *L. staplini* but contains small numbers of *Candona caudata*, *Cypridopsis vidua* and *Cyprideis beaconensis* in layers of diatomaceous clay, aragonite mud and organic matter silt indicating possible freshwater and/or groundwater discharge at the core site. Several horizons between 28 and 17 mblf (67,000±7000 to 25,000±2000 cal yr BP) suggest the core site was inundated by hypersaline water as indicated by the absence of all ostracodes and the presence of brine fly and brine shrimp fossils.

Our multivariate analysis indicates a shift from ‘shallow saline-water’ assemblages to ‘offshore freshwater’ assemblages takes place by ~16.59 mblf (25,000±2000 cal yr BP) when *Candona* (cf.) *caudata* and *Limnocythere staplini* become abundant. This is a freshwater assemblage of ostracodes because *C.* (cf.) *caudata* has extremely narrow salinity tolerances and is only associated with freshwater. *L. staplini* has very broad salinity tolerances and it indicates saline conditions only when it is found alone in this system. DCA results indicate full deep freshwater conditions at least by the time the 15.79 mblf sample was deposited (21,000±2000 cal yr BP), with its assemblage of abundant *Candona adunca* and *Limnocythere ceriotuberosa*. Unpublished studies of other piston cores from the lake indicate that this freshwater interval persisted from ~23,000–16,000 cal yr BP (~19,000–14,000 ^{14}C yr BP) (Oviatt, personal communication, 2004). Above the fresh open-water condition indicators, we have no ostracode record. Black sapropelic, unfossiliferous muds above this level may indicate a rapid decline in lake level because anoxic conditions are common in shallow water containing high salt concentrations. Sapropel accumulation appears to have started considerably earlier in this portion of the lake than in the southwest arm of the lake, where sapropel deposition began some time between 11,400 and 13,100 cal yr BP (Oviatt, personal communication, 2004, although uncertainties in our age model for this period make a precise age assignment for this transition at Site 4 difficult).

3.10. Zone F: 15.8–0 mblf (19,000–0 cal yr BP)

The presence of the upper salt (thenardite) layer (~14.4–8 mblf: 17,000±3000 to 11,000±4000 cal yr BP) indicates another rapid desiccation event followed by hypersaline conditions and authigenic evaporite precipitation. Black sapropelic muds are in layers within the salt crust. The lowest brine shrimp in this interval occur in zone F within an evaporite zone at 13.31 mblf (14,000±3000 cal yr BP) with the presence of brine shrimp eggs. Above the salt crust and sapropelic muds are pelleted aragonitic muds from 8 to 0 mblf (11,000±4000 cal yr BP to present) and with the exclusive presence of brine shrimp and brine fly fossils suggesting the lake has remained hypersaline throughout the Holocene.

4. Discussion

Although the record described in this study cannot be used to infer fine scale (decadal or centennial level) changes in lake history it does provides valuable insight into the broader behavior of this lake system over the past 280 ka at the millennial scale. For instance, in zones A–F, we see frequent alternations in lithofacies and biofacies between (1) saline/hypersaline open water indicators, (2) salt or freshwater marsh indicators or (3) offshore, deep freshwater indicators. These alternations provide strong evidence for fluctuating lake levels at the core site, and by extension, regional paleohydrology and climatic conditions. However, these cannot be interpreted simply as a sequence of wetter (3) to drier (1) conditions, as might be expected. To understand this fact it is instructive to consider the lateral facies variations observed around the Great Salt Lake today. Surrounding the current saline lake are numerous freshwater, spring or seepage fed marshes, forming at the groundwater discharge zone along the lake margin. Frequent small scale fluctuations in lake levels cause these marsh sites to be either flooded by the saline lake during rising lake levels, or converted into erosional or soil forming surfaces when lake level falls and the marshes migrate basinwards. Thus, a vertical sequence of sediments representing a transition from highest lake levels to lowest in this context is represented by a) deep water deposits and relatively freshwater indicators, to b) shallower, but still offshore, saline lake indicators, when the site is still fully submerged to c) saline marsh (lake margin) indicators as the site approaches the lake surface level, to d) freshwater marsh indicators (lake level slightly below core site, spring or fluvial discharge), to e) paleosols and erosion surfaces when lake level is well below the core site (Fig. 6B). Similarly, evaporite deposits should not be thought of as representative of the lowest/driest lake conditions. More probably they form at times when the dissolved solid budget of a large and deep lake is undergoing its most rapid brine concentration. Textural evidence from Site 4's evaporites also suggests they formed subaqueously, analogous to the salts of rapidly concentrating brines in other ancient and modern hypersaline lakes (e.g. Li et al., 1996; Krumgalz, 1997). The volume/thickness of evaporite sequences in the Great Salt Lake is therefore strongly linked to the volume of the antecedent waterbody (i.e., lower preceding highstands will yield smaller evaporite bodies upon evaporite precipitation).

4.1. Site 4 and global climate change

Both conceptual and General Circulation Models (GCM) have predicted that a southward diversion of the jet stream during glacial maxima would have a major impact on precipitation/evaporation ratios in the eastern Great Basin (Antevs, 1948; COHMAP, 1988; Thompson et al., 1993). The record of lake level oscillations contained in Site 4 is in agreement with GCM predictions and show that the system has been strongly influenced by climate forcing over the last four glacial/interglacial sequences. We have compared the marine OIS chronology (Martinson et al., 1987) with the timing of local lake oscillations. Given the inherent uncertainties of our age model, our results are consistent with the hypothesis that that the pattern of paleohydrological change recorded in the sediments of Site 4 was largely controlled by global changes in climate (Fig. 6A).

4.2. MID OIS 8.4–OIS 7.0 (280,000–190,000 yr BP)

Although lake levels oscillate considerably during this stage, overall they tend to decrease. Our record begins in mid OIS 8.4 at 280,000±30,000 yr BP, when the basin contained a shallow saline lake (zone

A, bottom) but quickly became hypersaline (zone A, middle). This does not necessarily indicate that lake level decreased, but it does suggest a higher brine concentration. There are good indications, however, that evaporation was causing lake levels to decrease because by 260,000±30,000 yr BP (beginning of stage 8.4), lake levels were at/below the core site and marsh conditions began to dominate (bottom of zone B). Extensive marshes with periodic soil formation (zone B 250,000±30,000 to 230,000±20,000 yr BP) correlate with SPECMAP's very high peak around the transition from OIS 8 to OIS 7. Lake levels increase to deeper saline/hypersaline conditions during OIS 7.4 when global ice volume slightly increases. The lake remains saline/hypersaline as global ice volume decreased to relatively low levels from OIS 7.4–7.3. When global ice volume increases again during OIS 7.2–7.3, we see lake level dropping slightly below the core site as evidenced by a highly diverse freshwater marsh community at 91–90 mblf (220,000–210,000±20,000 yr BP). However, we have evidence of delta progradation at the core site immediately before this time period (~220,000±20,000 yr BP) and therefore, lake levels may appear more shallow at this time due to sediment progradation rather than a climate-driven decrease in lake level. As global ice volume increases during OIS 7.1–7.0 we see lake levels rising again and inundating the core site causing hypersaline conditions (zone C, middle).

4.3. OIS 6 (190,000–130,000 yr BP)

Lake levels fluctuate primarily between saline and hypersaline conditions throughout this glacial cycle, although there is evidence of one deep freshwater lake cycle. Transgression of lake levels from shallow saline to deep freshwater by 170,000±20,000 yr BP is suggested by the in situ freshwater ostracodes found in zone C. The age of this potentially deep freshwater lake correlates with the timing of the Little Valley lake cycle, independently dated at ~150,000 yr BP based on amino acid dating of gastropod shells from a lacustrine sand in Little Valley (Scott et al., 1983; Oviatt et al., 1999). Through close interval sampling of the Little Valley sediments, Oviatt et al. (1999) were able to tightly constrain the highest and freshest stand conditions of that lake cycle, an event that was missed by our coarser-interval sampling.

The lower salt crust was deposited directly above the deep freshwater deposits, but at our level of resolution, the lower evaporite (halite) layer in zone C may have been deposited anytime between OIS 6.5 and 6.3 (~183,000–142,000 yr BP). Assuming the freshwater deposits are from the Little Valley lake cycle, we can constrain the age of the evaporite to ~170,000–140,000 yr BP. Even with the constrained date, the age of the lower salt crust places its deposition at the same time as when global ice volume was at its highest during the OIS 6 glaciation. Therefore, our records indicate the region experienced heavy precipitation as global ice volume increased close to its maximum and then a rapid change in climate led to highly evaporative conditions during the OIS 6 glacial maximum. As with the last glacial maximum (OIS 2), the OIS 6 glacial maximum might be predicted to bring greater precipitation to this part of the Great Basin, which is in partial agreement with our study. However, the highly evaporative conditions at the height of the glaciation may be better correlated with regional climate controls (i.e., movement of alpine glaciers or the North American ice sheet).

After evaporite deposition, many small lake level oscillations occurred in the basin causing an alternation in environments at the core site from shallow saline to hypersaline conditions. During OIS 6.0–OIS 5.5 (the highest and warmest peak) lake level decreased to the point of subaerial exposure at the core site (zone D:130,000±10,000 yr BP).

4.4. OIS 5 (130,000–74,000 yr BP)

Lake levels increase slightly around 130,000±10,000 yr BP but fell once again within about 2000 yr to levels slightly below/at the core site as indicated by the extreme marsh conditions (zone D). Marsh conditions and therefore, low lake levels prevail through much of this interglacial however, periodic increases in lake level from 100,000±10,000 to 95,000±10,000 yr BP and 84,000±9000 to 73,000±8000 yr BP correspond to the lower (cooler) peaks of OIS 5.0–5.1 and OIS 5.2–5.3, respectively.

4.5. OIS 4 (74,000–59,000 yr BP)

The environmental conditions at the core site throughout most of this glacial cycle were, in large

part, saline to hypersaline (zone E). Abundant *Limnocythere staplini* from 71,000±8000 to 67,000 ±7000 yr BP are followed by intervals with abundant brine shrimp/fly fossils and no *L. staplini* (65,000 to 62,000 yr BP). Again, this shift from saline conditions to hypersaline conditions does not necessarily indicate a drop in lake level but instead may have been simply a response to the buildup of dissolved salts over time. At the OIS 4/OIS 3 transition we have evidence of an open saline lake with a low abundance of *L. staplini* and a few brine shrimp fecal pellets (60,000±6000 yr BP). The U-series-based model age of this saline lake corresponds closely with the independently published age of 59,000±5000 yr BP for the Cutler Dam Alloformation based on amino acid racemization (Kaufman et al., 2001). Our results suggest that the Cutler Dam lake cycle did not include a deep freshwater interval, which is consistent with both shoreline studies that indicate the upper limit of the lake at this time was significantly lower than the highest levels of the Bonneville or Little Valley lake cycles, probably no higher than 1370 m (Oviatt et al., 1987; Kaufman et al., 2001). Prior paleoecological studies of ostracodes from this time period also suggests a saline lake was present even at the lake's highest stand (Oviatt et al., 1987). The lower magnitude of OIS 4 glaciation might be predicted to bring less precipitation to the basin and therefore, lower lake levels than those associated with either the stage 6 (Little Valley) or the stage 2 (Bonneville) events (Oviatt et al., 1987; Kutzbach et al., 1994; Kaufman et al., 2001). Additionally, there is some evidence indicating that the upper Bear River (a major tributary) was not flowing into the catchment at this time (Oviatt et al., 1987). Our study is in agreement with Kaufman et al. (2001) who indicated the maximum highstand for Cutler Dam occurred following the peak in OIS 4 (see Fig. 6A).

4.6. OIS 3–OIS 2 (59,000–12,000 cal yr BP)

Throughout most of interglacial OIS 3, lake levels remained fairly low and oscillated between shallow saline and hypersaline conditions at the core site (zone E). Site 4 records the presence of a deep freshwater lake in the basin from 25,000±2000 to 21,000±2000 cal yr BP (transition from OIS 3 to OIS 2), corresponding to deposition of finely laminated, variegated silty clays and carbonate muds. The *Candona adunca*/*Limnocythere ceriotuberosa* assemblage at the top of zone E (21,000±2000 cal yr BP) correlates this deep freshwater lake to the middle transgressive phase of Lake Bonneville (Thompson et al., 1990; Oviatt et al., 1992, Oviatt, personal communication, 2004). The upper evaporite (thenardite) layer (zone F) was deposited sometime between 17,000±3000 and 11,000±3,000 cal yr BP according to our age model. This is consistent with the post-Provo regressive phase of Lake Bonneville, when overflow ceased and the basin became hydrologically closed once again (Oviatt et al., 1992). The termination of Lake Bonneville's overflow phase is not well established from shoreline evidence but probably lies in the range of 17,000–14,500 cal yr BP (13.5–13.0 ka ^{14}C yr BP), which is consistent with our age model. It is important to note however that the detailed chronology of events known from the Bonneville and post-Bonneville phases of the GSL record from many other locations cannot be compared event–by-event with the lower resolution Site 4 record described here.

4.7. OIS 1 (12,000–0 cal yr BP)

Since the early Holocene, lake levels have remained low and hypersaline conditions have prevailed in the Great Salt Lake basin. Our study was at too low of a resolution to capture the Gilbert shoreline complex or any of the small lake level oscillations that are discussed in Currey (1990).

4.7.1. Comparison with other lake records

Physical, chemical and biological records from lakes and paleolakes in the western United States have often been compared to elucidate the role of climate change in regional environmental variation (i.e., Benson and Thompson, 1987; Morrison, 1991; Thompson et al., 1993). The vast majority of these studies have focused on the last glacial advance (i.e., OIS2), since many high-resolution records with excellent chronological control exist for that time period (i.e., Oviatt et al., 1992). Our study is at too low of a resolution to adequately compare our record of environmental change during the OIS 2 glaciation with these high-resolution studies. Instead, we will

focus our regional comparison on the older, and less understood, OIS 6 and OIS 4 intervals.

OIS 6 was marked by dry conditions in the Bonneville basin, given the majority of lake fluctuations during OIS6 were between saline/hypersaline and marsh environments. One major exception is for the period immediately before the glacial maximum when the Bonneville basin may have received heavy precipitation, as evidenced by the Little Valley Highstand deposits, ~167,000 yr BP. Highly dry/evaporative conditions prevailed soon after the Little Valley and a thick evaporite was deposited during the glacial maximum, according to our chronology. In comparison, records from Summer Lake, Oregon show a lake highstand and a progressively moister climate occurring much earlier than in the Bonneville basin (Cohen et al., 2000). Deposits from Summer Lake cores and outcrops provide evidence of higher lake levels and cooler temperatures from 236,000 to 165,000 yr, although there is evidence of a brief reversal towards more saline (i.e., possibly drier) conditions ~200,000 yr ago (Cohen et al., 2000). By 165,000 yr ago, most of the Summer Lake data point to drier and warmer conditions, which correlates with the age of our lower evaporite deposit. Ancient Lake Manly located in the Badwater Basin, Death Valley, CA contains deposits that suggest an increase in moisture (via increased water input) throughout OIS 6 glaciation (Lowenstein, 2002). From 200,000 to 192,000 yr ago, the area contained extensive mudflats but from 192,000 to 186,000 yr ago, increased water input led to the existence of ephemeral saline lakes. Deeper perennial lakes occurred from 186,000 to 120,000 yr ago, which fluctuated between fresh and saline waters, but by 120,000 yr ago (OIS 5) drier conditions prevailed and the lake was reduced to mud flats (Lowenstein, 2002).

Records from Summer Lake, Death Valley and our study of the Bonneville basin indicate dry/arid conditions prevailed during the OIS 5 interglacial. Devil's Hole, Nevada (Szabo et al., 1994) shows a drop in the water table between 116,000 and 104,000 yr ago, around the same time our record shows a decrease in lake level from a salt marsh to a freshwater marsh. Records from Carp Lake in the Columbia basin, Washington, also indicate warm and dry conditions with open forest dominating the landscape at OIS 5.5 (5e) and mainly cool/dry conditions dominating most of the interglacial (Whitlock et al., 2000). Records from Summer Lake, Carp Lake and our study of the Bonneville basin indicate regionally moister climate throughout the northern Great Basin beginning around OIS 5.1 (5e) and continues through OIS 4. All proxies from the Summer Lake study indicate moister climates from 89,000 to 50,000 yr ago, although deviations from this are suggested by several warming excursions in the palynological data (Cohen et al., 2000). Pollen studies from Carp Lake indicate open forest environments and a warm/humid climate from 85,100 to 73,900 yr ago (Whitlock et al., 2000). Our study indicates lake levels increasing from saline marsh to shallow/offshore saline conditions by ~83,700 yr BP which continues with little variation throughout the OIS 4 interval (Fig. 6). Somewhat wetter periods in climate were not present in Death Valley until 60,000 yr ago, when ephemeral saline lake sediments were deposited over mudflat deposits (Lowenstein, 2002). Higher than average water table levels were not recorded in Devil's Hole, Nevada until 44,000–20,000 yr ago (OIS 3–OIS 2).

Climate models hindcasting changes in climate during the OIS 2 glaciation indicate somewhat coherent patterns in climate throughout the western United States, with regional variations in lake–atmosphere interactions, effective moisture, temperature and solar insolation (Hostetler et al., 1994; Thompson et al., 1993). Our comparison between OIS 6 records from around the western United States show a similar result, in that the overall pattern of climate was similar in the regions, but differences in the timing of climate changes (i.e., when a region became drier or moister) are common.

5. Conclusion

Site 4 contains a highly continuous paleoecological archive of Quaternary environmental and climate change. Our intermediate resolution sampling (~2,000 yr) is too coarse to capture the finer environmental fluctuations preserved in the core, however this study is a first step in unlocking the rich paleoenvironmental story of the Bonneville basin preserved at Site 4. Its paleoecological and sedimentological indicators show that the core site has fluctuated over time mostly between marsh and saline to hypersaline open-water conditions, but has, on occasion, been

submerged in deep, freshwater. These local environmental changes can be understood in terms of oscillating lake levels. Our study confirms that climate forcing has played a major role in these lake level fluctuations and some, though not all, of the climatic fluctuations can be associated with changes in global ice volume. Overall, we see low to very low lake levels during the interglacial cycles (OIS 7, 5, 3 and 1). The lowest lake levels coincide with the presence of marsh indicators in the core's sedimentary and paleoecological record. Saline/hypersaline conditions at the core site indicate regional lake levels higher than during marsh phases, but significantly lower than open freshwater conditions, such as the Little Valley cycle (mid OIS 6) and the Lake Bonneville cycle (late OIS 2). However, the climate of the Great Salt Lake catchment appears to have been drier during OIS 6 than during OIS 2. Thus, the high-resolution records and climate models from the last glacial advance may not serve as a good analog for the older glacial cycles. Many smaller lake level oscillations are recorded in Site 4, and with higher resolution sampling and a more robust age model, we may find that these smaller oscillations are sensitive to climate changes on millennial or shorter time scales. Oviatt (1997) found that some of the lake fluctuations associated with Lake Bonneville coincided with millennial scale Heinrich events.

The sediments contained in Site 4 provide a detailed natural archive of (1) local environmental and ecological change at the core site (2) fluctuations in regional paleohydrology and (3) climate change over the last four glacial/interglacial sequences. This long, continuous record provides important insights into the paleoecology, paleohydrology and paleoclimate of the northeastern Great Basin, and will allow us the unique opportunity to link these insights into an interdisciplinary framework of past global change.

Acknowledgements

The authors wish to gratefully acknowledge several people. A special thanks to DOSECC and their drilling crew, for without them, this study would not have been possible. We also wish to thank Rick Forester and Manuel Palacios-Fest for invaluable help with ostracode taxonomy and ecology; Jack Oviatt for generously sharing his knowledge of and unpublished data on the history of the Great Salt Lake. We also thank Jack Oviatt and Rick Forester for their insightful reviews of an earlier version of the manuscript. We also thank Todd Lange for his assistance with radiocarbon dating, Karen Bossenbroek for her work on brine fly proleg fossils, and Kaustuv Roy for helpful discussions and use of his lab facilities during the Summer 2002. This research was generously supported by NSF grant ESH-9905168 to A.C., NSF grant MRI-0116395 to R.L.E., NSF grant EAR-0001120 to DOSECC for drilling operations and a Summer 2002 internship to D.B. provided by DOSECC. We dedicate this paper to the memory of Kerry Kelts, without whose tireless promotion of the global lakes drilling (GLAD) program in general, and the pilot drilling at the Great Salt Lake in particular, this research project would not have been possible.

References

Antevs, E., 1948. Climatic changes and pre-white man. The Great Basin, with Emphasis on Glacial and Postglacial Times, Bulletin of the University of Utah, vol. 38, pp. 167–191.

Beck, W.J., Richards, D.A., Edwards, R.J., Silverman, B.W., Smart, P.L., Donahue, D.J., Hererra-Osterheld, S.H., Burr, G.S., Calsoyas, L., Jull, A.J.T., Biddulph, D., 2001. Extremely large variations of atmospheric ^{14}C concentration during the last glacial period. Science, 292, 2453–2458.

Benson, L.V., Thompson, R.S., 1987. The physical record of lakes in the Great Basin. In: Ruddiman, W.F., Wright Jr., H.E. (Eds.), The Geology of North America. North America and Adjacent Oceans During the Last Deglaciation, vol. K-3. Geol. Soc. Am., Boulder, CO, pp. 241–260.

Cheng, H., Edwards, R.L., Hoff, J., Gallup, C.D., Richards, D.A., Asmerom, Y., 2000a. The half-life of uranium-234 and thorium-230. Chem. Geol., 169, 17–33.

Cheng, H., Adkins, J.F., Edwards, R.L., Boyle, E.A., 2000b. ^{230}Th dating of deep-sea corals. Geochim. Cosmochim. Acta, 64, 2401–2416.

Cobb, K.M., Charles, C.D., Cheng, H., Edwards, R.L., Kastner, M., 2003. U/Th-dating living and young fossil corals from the central tropical Pacific. Earth Planet. Sci. Lett., 210, 91–103.

Cohen, A.S., Palacios_Fest, M.R., Negrini, R.M., Wigand, P.E., Erbes, D.B., 2000. A paleoclimate record for the past 250,000 years from Summer Lake, Orgeon, USA: II. Sedimentology, paleontology and geochemistry. J. Paleolimnol., 24, 151–182.

COHMAP, 1988. Climate changes in the last 18,000 years: observations and simulations. Science, 241, 1043–1052.

Currey, D.R., 1990. Quaternary palaeolakes in the evolution of semidesert basins, with Special emphasis on Lake Bonneville and the Great Basin, USA. Palaeogeogr. Palaeoclimatol. Palaeoecol., 76, 189–214.

Currey, D.R., Oviatt, C.G., 1985. Durations, average rates, and probable causes of Lake Bonneville expansions, still-stands, and contractions during the last deep-lake cycle, 32,000 to 10,000 years ago. In: Kay, P.A., Diaz, H.F. (Eds.), Problems of and Prospects for Predicting Great Salt Lake Level. Cent. Publ. Affairs Admin. Univ. Utah, pp. 9–24.

Davis, O.K., 1998. Palynological evidence for vegetation cycles in a 1.5 million year pollen record from the Great Salt Lake, Utah, USA. Palaeogeogr. Palaeoclimatol. Palaeoecol., 138, 175–185.

Davis, O.K., Moutoux, T.E., 1998. Tertiary and Quaternary vegetation history of the Great Salt Lake. J. Paleolimnol., 19, 417–427.

Dean, W., Rosenbaum, J., Haskell, B., Kelts, K., Schnurrenberger, D., Valero-Garces, Blas, Cohen, A., Davis, O., Dinter, D., Nielson, D., 2002. Progress in global lake drilling holds potential for global change research. Trans.-Am. Geophys. Union, 83 (85), 90–91.

Delorme, L.D., 1970a. Freshwater ostracodes of Canada: Part I. Subfamily cypridinae. Can. J. Zool., 48, 153–168.

Delorme, L.D., 1970b. Freshwater ostracodes of Canada: Part II. subfamilies cypridopsinae and herpetocypridinae, and family cyclocyprididae. Can. J. Zool., 48, 253–266.

Delorme, L.D., 1970c. Freshwater ostracodes of Canada: Part III. Family candonidae. Can. J. Zool., 48, 1099–1127.

Delorme, L.D., 1970d. Freshwater ostracodes of Canada: Part IV. Families ilyocyprididae, notodromadidae, darwinulidae, cytheridae, entocytheridae. Can. J. Zool., 48, 1251–1259.

Delorme, L.D., 1971. Freshwater ostracodes of Canada: Part V. Families limnocytheridae, loxoconchidae. Can. J. Zool., 49, 43–64.

Delorme, L.D., 1991. Ostracoda. In: Thorp, J., Covich, A. (Eds.), Ecology and Classification of North American Freshwater Invertebrates. Academic Press, San Diego, pp. 691–721.

Edwards, R.L., Chen, J.H., Wasserburg, G.J., 1987. ^{238}U–^{234}U–^{230}Th–^{232}Th systematics and the precise measurement of time over the past 500,000 years. Earth Planet. Sci. Lett., 81, 175–192.

Forester, R.M., 1983. Relationship of two lacustrine ostracode species to solute composition and salinity: implications for paleohydrochemistry. Geology, 11, 435–438.

Forester, R.M., 1985. Limnocythere bradburyi n.sp.: a modern ostracode from Central Mexico and a possible Quaternary paleoclimatic indicator. J. Paleontol., 59, 8–20.

Forester, R.M., 1986. Determination of the dissolved anion composition of ancient lakes from fossil ostracodes. Geology, 14, 796–798.

Forester, R.M., 1987. Late Quaternary paleoclimate records from lacustrine ostracodes. In: Ruddiman, W.F., Wright, H.E. (Eds.), The Geology of North America, North America and Adjacent Oceans During the Last Deglaciation, vol. K-3. Geol. Soc. of Am., Boulder, CO, pp. 261–276.

Forester, R.M., 1991a. Ostracode assemblages from springs in the western United States: implications for paleohydrology. Mem. Entomol. Soc. Can., 155, 181–201.

Forester, R.M., 1991b. Pliocene-climate history of the Western United States derived from lacustrine ostracodes. Quat. Sci. Rev., 10, 133–146.

Forester, R.M., Brouwers, E.M., 1985. Hydrochemical parameters governing the occurrence of estuarine and marginal estuarine ostracodes: an example from south-central Alaska. J. Paleontol., 59, 344–369.

Forester, R.M., Colman, S.M., Reynolds, R.L., Keigwin, L.D., 1994. Lake Michigan's late Quaternary limnological and climate history from ostracodes, oxygen isotopes and Magnetic susceptibility. J. Great Lakes Res., 20, 93–107.

Gilbert, G.K., 1890. Lake Bonneville. U.S. Geological Survey Monograph, vol. 1. US Printing Office, Washington, DC.

Holmes, J.A., Chivas, A.R. (Eds.), 2002. The Ostracoda: Applications in Quaternary Research. American Geophysical Union, Washington, DC.

Hostetler, S.W., Giorgi, F., Bates, G.T., Bartlein, P.J., 1994. Lake–atmosphere feedbacks associated with paleolakes Bonneville and Lahontan. Science, 263, 665–668.

Kaufman, D.S., Forman, S.L., Bright, J., 2001. Age of the Cutler Dam Alloformation (late Pleistocene), Bonneville basin, Utah. Quat. Res., 56, 322–334.

Kitagawa, H., van der Plicht, J., 1998. Atmospheric radiocarbon calibration to 45,000 yr B.P.: late glacial fluctuations and comogenic isotope production. Science, 279, 1187–1190.

Kowalewska, A., Cohen, A.S., 1998. Reconstruction of paleoenvironments of the Great Salt Lake Basin during the late Cenozoic. J. Paleolimnol., 20, 381–407.

Krumgalz, B.S., 1997. Ion interaction approach to geochemical aspects of the Dead Sea. In: Niemi, T.M., Ben-Avraham, Z., Gat, J.R. (Eds.), The Dead Sea: The Lake and Its Settings. Oxford Monographs on Geology and Geophysics, vol. 36. Oxford University Press, New York, pp. 145–160.

Kutzbach, J.E., Guetter, P.J., Behling, P.J., Selin, R., 1994. Simulated climatic changes: results of the COHMAP climate-model experiments. In: Wright Jr., H.E., Kutzbach, J.E., Webb, T.I., Ruddiman, W.T., Street-Perrott, F.A., Bartlein, P.J. (Eds.), Global Climates Since the Last Glacial Maximum. University of Minnesota, Minneapolis, pp. 24–93.

Li, J., Lowenstein, T.K., Brown, C.B., Teh-Lung, K., Luo, S., 1996. A 100 ka record of water tables and paleoclimates from salt cores, Death Valley, California. Palaeogeogr. Palaeoclimatol. Palaeoecol., 123, 179–203.

Lin, J.C., Broecker, W.S., Anderson, R.F., Hemming, S., Rubenstone, J.L., Bonani, G., 1996. New $^{230}Th/U$ and ^{14}C ages from Lake Lahontan carbonates, Nevada, USA, and a discussion of the origin of initial thorium. Geochim. Cosmochim. Acta, 60, 2817–2832.

Lowenstein, T.K., 2002. Pleistocene lakes and paleoclimates (0 to 200 Ka) in Death Valley, California. In: Hershler, R., Madsen, D.B., Currey, D.R. (Eds.), Great Basin Aquatic Systems History. Smithsonian Contributions to the Earth Sciences, vol. 33. Smithsonian Institution Press, Washington, DC, pp. 109–120.

Martinson, D.G., Pisias, N.G., Hays, J.D., Imbrie, J., Moore, T.C., Shackleton, N.J., 1987. Age dating and the orbital theory of the ice ages: development of a high resolution 0 to 300,000 year chronostratigraphy. Quat. Res., 27, 1–29.

Morrison, R.B., 1991. Quaternary stratigraphic, hydrologic and climatic history of the Great Basin, with emphasis on Lakes Lahontan, Bonneville and Tecopa. In: Morrison, R.B. (Ed.),

Quaternary Nonglacial Geology: Conterminous U.S. The Geology of North America, vol. K-2. Geological Society of America, Boulder, CO, pp. 283–320.

Oviatt, C.G., 1997. Lake Bonneville fluctuations and global climate change. Geology, 25, 155–158.

Oviatt, C.G., 2002. Bonneville basin lacustrine history: the contributions of G.K. Gilbert and Ernst Antevs. In: Hershler, R., Madsen, D.B., Currey, D.R. (Eds.), Great Basin Aquatic Systems History. Smithsonian Contributions to the Earth Sciences, vol. 33. Smithsonian Institution Press, Washington, DC, pp. 121–129.

Oviatt, C.G., McCoy, W.D., Reider, R.G., 1987. Evidence for a shallow Early or Middle Wisconsin-age lake in the Bonneville basin, Utah. Quat. Res., 2, 248–262.

Oviatt, C.G., Currey, D.R., Miller, D.M., 1990. Age and paleoclimatic significance of the Stansbury shoreline of Lake Bonneville, northeastern Great Basin. Quat. Res., 33, 291–305.

Oviatt, C.G., Currey, D.R., Sack, D., 1992. Radiocarbon chronology of Lake Bonneville, Eastern Great Basin, USA. Palaeogeogr. Palaeoclimatol. Palaeoecol., 99, 225–241.

Oviatt, C.G., Thompson, R.S., Kaufman, D.S., Bright, J., Forester, R.M., 1999. Reinterpretation of the Burmester Core, Bonneville Basin, Utah. Quat. Res., 52, 180–184.

Palacios, M., Cohen, A., Haskell, B., Valero-Garces, B., Schnurrenberger, D., Heil, C., Dean, W., Davis, O., Kruger, N., Dinter, D., 2001. GLAD 1, GSL Site 4. In: Schnurrenberger, D., Haskell, B. (Eds), Initial Reports of Global Lakes Drilling Program Volume 1. Glad 1: Great Salt Lake, Utah and Bear Lake, Utah, Idaho. Limnological Research Center CDROM, University of Minnesota, Minneapolis, Minnesota, pp. 37–46; 271–315.

Palacios-Fest, M., Cohen, A.S., Anadon, P., 1994. Use of ostracodes as paleoenvironmental tools in the interpretation of ancient lacustrine records. Rev. Esp. Paleontol., 9, 145–164.

Renaut, R., Last, W. (Eds.), 1994. Sedimentology and Geochemistry of Modern and Ancient Saline Lakes. SEPM Spec. Publ., vol. 50.

Schnurrenberger, D., Russell, J., Kelts, K., 2003. Classification of lacustrine sediments based on sedimentary components. J. Paleolimnol., 29, 141–154.

Scott, W.E., McCoy, W.D., Shroba, R.R., Rubin, M., 1983. Reinterpretation of the exposed record of the last two cycles of Lake Bonneville, western United States. Quat. Res., 20, 261–285.

Shen, C.C., Edwards, R.L., Cheng, H., Dorale, J.A., Thomas, R.B., Moran, S.B., Weinstein, S.E., Hirschmann, M., 2002. Uranium and thorium isotopic and concentration measurements by magnetic sector inductively coupled plasma mass spectrometry. Anal. Chem., 185, 165–178.

Smith, A.J., 1993a. Lacustrine ostracodes as hydrochemical indicators in lakes of the north-central United States. J. Paleolimnol., 8, 121–134.

Smith, A.J., 1993b. Lacustrine ostracode diversity and hydrochemistry in lakes of the northern Midwest of the United States. In: McKenzie, K.G., Jones, P.J. (Eds.), Ostracoda in the Earth and Life Sciences. Ashgate Pub. Co. Balkema, Rotterdam. pp. 493–500.

Smith, A.J., Delorme, L.D., Forester, R.M., 1992. A lake's solute history from ostracodes: comparison of methods. In: Kharaka, Y.K., Maest, A.S. (Eds.), Rock–Water Interaction: Proceedings of the 7th International Symposium Water–Rock Interaction, Park City, Utah, pp. 677–680.

Spencer, R.J., Baedecker, M.J., Eugster, H.P., Forester, R.M., Goldhaber, M.B., Jones, B.F., Kelts, K., Mckenzie, J., Madsen, D.B., Rettig, S.L., Rubin, M., Bowser, C.J., 1984. Great Salt Lake, and precursors, Utah: the last 30,000 years. Contrib. Mineral. Petrol., 86, 321–334.

Szabo, B.J., Kolesar, P.T., Riggs, A.C., Winograd, I.J., Ludwig, K.R., 1994. Paleoclimatic inferences from a 120,000-yr calcite record of water-table fluctuation in Browns Room of Devils Hole, Nevada. Quat. Res., 41, 59–69.

ter Braak, C.J.F., Prentice, I.C., 1988. A theory of gradient analysis. Adv. Ecol. Res., 18, 271–317.

ter Braak, C.J.F., Smilauer, P., 1998. CANOCO Reference Manual and User's Guide to CANOCO for Windows (Version 4). Microcomputer Power, Ithaca, NY. 352 pp.

Thompson, R.S., Toolin, L.J., Forester, R.M., Spencer, R.J., 1990. Accelerator-mass spectrometer (AMS) radiocarbon dating of Pleistocene lake sediments in the Great Basin. Palaeogeogr. Palaeoclimatol. Palaeoecol., 78, 301–313.

Thompson, R.S., Whitlock, C., Bartlein, P.J., Harrison, S.P., Spaulding, W.G., 1993. Climatic changes in the western United States since 18,000 yr B.P. In: Wright Jr., H.E., Kutzbach, J.E., Webb, T.I., Ruddiman, W.T., Street-Perrott, F.A., Bartlein, P.J. (Eds.), Global Climates Since the Last Glacial Maximum. University of Minnesota, Minneapolis, pp. 468–513.

Whitlock, C., Sarna-Wojcicki, A.M., Bartlein, P.J., Nickmann, R.J., 2000. Environmental history and tephrostratigraphy at Carp Lake, southwestern Columbia basin, Washington, USA. Palaeogeogr. Palaeoclimatol. Palaeoecol., 155, 7–29.

Zdanowicz, C.M., Zielinski, G.A., Germani, M.S., 1999. Mount Mazama eruption: calendrical age verified and atmospheric impact assessed. Geology, 27, 621–624.